TAMPEREEN TEKNILLINEN YLIOPISTO
TAMPERE UNIVERSITY OF TECHNOLOGY

PASI PEIJARINIEMI

DESIGN OF EXPERIMENT APPLIED TO TRANSMISSION LINES IN RADIO FREQUENCY NETWORK SIMULATIONS

Master of Science thesis

Examiners: prof. Mikko Valkama
and D.Sc. (Tech.) Olli-Pekka Lunden
Examiner and topic approved by the Faculty Council of the Faculty of Computing and Electrical Engineering on 3th June 2015

ABSTRACT

PASI PEIJARINIEMI: Design of Experiment Applied to Transmission Lines in Radio Frequency Simulations
Tampere University of Technology
Master of Science Thesis, 50 pages
June 2015
Master's Degree Programme in Electrical Engineering
Major: Wireless Communications
Examiner: Professor Mikko Valkama and D.Sc. (Tech.) Olli-Pekka Lunden

Keywords: RF, Transmission lines, Design of Experiment

Design of experiment is a method where the relation between input factors and outputs can be studied. In practice, a number of experiments are conducted and the input(s) are changed between each experiment. Gained information can then be used to find out how to improve the process under study. It is applicable to many areas from cooking to radio frequency (RF) simulations. This thesis focuses on the effects of transmission line lengths and their effect to different RF parameters. Study is applied to a long term evolution frequency division duplexing (LTE-FDD) mobile front end. The purpose is to find out the applicability of DOE to RF design process.

To be able to start final simulations it is required that layout is completed. When layout is finished, accurate parameter values can be used to receive reliable results. For example, transmission line lengths are acquired from the layout. However, there may be situations where the layout is not entirely finished. Therefore, it would be an advantage if limits for the length of a transmission line length could be defined without compromising reliability. In this thesis DOE is applied to search for suitable limits for the transmission line lengths. If applicable boundaries are found, simulations could be done before layout is completed.

To find out the acceptable boundaries, existing simulation models are used to study the effects of transmission line lengths to different RF parameters. Chosen transmission lines are then varied in length with desired limits. Acquired results, using the limits, are then compared to a nominal case, where no transmission line variation is done. A set of different percentual limits are used. Studied RF parameters are insertion loss and return losses in each port.

DOE was utilized on two RF (LTE-FDD) front ends. LTE-FDD bands 2 and 12 were chosen to cover two unique cases. Though only LTE-FDD front ends are investigated, the information received could also be applied on other RF transmission lines in other types of front end, such as GSM or WCDMA front ends.

The study revealed that DOE can be used as tool to evaluate whether a transmission line length, within a limit, is applicable to continue simulation process. In some situations the case might be that no applicable limit is found. If the limit is not usable, simulation process cannot be continued without compromising the accuracy of the results.

TIIVISTELMÄ

PASI PEIJARINIEMI: Koesuunnittelun soveltaminen siirtolinjoihin radiotaajuus simuloinneissa
Tampereen teknillinen yliopisto
Diplomityö, 50 sivua
Kesäkuu 2015
Sähkötekniikan diplomi-insinöörin tutkinto-ohjelma
Pääaine: Wireless Communications
Tarkastaja: professori Mikko Valkama ja (TkT) Olli-Pekka Lunden

Avainsanat: RF, Transmission lines, Siirtolinjat, Design of Experiment, Koesuunnittelu

Koesuunnittelu on menetelmä, jolla voidaan tutkia muuttujien (input factor) ja ulostulojen (output) välistä vuorovaikutusta. Käytännössä tehdään sarja kokeita ja kokeiden välillä muuttujien arvoja muutetaan. Koesuunnittelua voidaan soveltaa moneen osa-alueeseen aina ruuanlaitosta RF simulointeihin. Tässä työssä keskitytään siirtolinjojen vaikutukseen long term evolution (LTE) piirissä erilaisiin tutkittuihin ulostuloihin. Tavoitteena on selvittää voidaanko koesuunnittelua hyödyntää helpottamaan suunniteluprosessia.

Tällä hetkellä on syytä odottaa, että elektroninen pohjapiirustus (layout) on valmis ennen viimeisten simulointien alottamista, jotta voidaan maksimoida simulointien tarkkuus. Esimerkiksi siirtolinjojen pituudet saadaan pohjapiirustuksesta. Voi kuitenkin olla tilanteita, jolloin pohjapiirustus ei ole vielä täysin valmis. Olisi hyödyksi, jos siirtolinjojen pituus voitaisiin määritellä tiettyjen rajojen sisälle, niin että simulointi tuloksiin voitaisiin yhä luottaa. Tässä työssä koesuunnittelua hyödynnetään sopivien rajojen etsimiseen. Jos sopivat rajat löydetään, olisi simuloinnit mahdollista aloittaa jo ennen kuin pohjapiirrustus on täysin valmis.

Tässä työssä on hyödynnetty olemassa olevia simulointia malleja, joiden avulla siirtolinjojen pituuksien vaikutuksia on tutkittu eri suorituskykyyn viittaaviin parametreihin. Siirtolinjojen pituutta varioidaan ennalta määrättyjen rajojen mukaisesti ja tuloksia verrataan tilanteeseen, jossa siirtolinjat ovat nominaalipituudessaan. Kolmea eri prosentuaalista arvoa on käytetty raja-arvoina. Siirtolinjojen pituuden vaikutusta tutkitaan impedanssi sovituksiin sekä vaimennukseen.

Koesuunnittelua sovellettiin kahteen eri LTE piiriin. Tutkimuskohteiksi valittiin taajuusalueet 2 ja 12, jotta voidaan tutkia kahta erilaista tapausta. Vaikka tutkimusta toteutetaan vain LTE piireillä, voidaan tutkimustuloksia hyödyntää esimerkiksi myös GSM ja WCDMA piireissä.

Huomattiin, että koesuunnittelua voidaan käyttää hyväksi varmistamaan onko tietyn rajan sisälle arvioidun siirtolinjan pituutta mahdollista käyttää simulointiprosessin

jatkamiseen. Joissakin tapauksissa voi kuitenkin käydä niin, että arvioidut rajat eivät ole riittäviä. Jos tarkkuus ei ole riittävä, ei simulointeja pystytä jatkamaan luotettavasti. Rajoittava tekijä koesuunnittelun toteutuksessa tämän kaltaisessa tapauksessa on rajojen soveltuvuus käytännössä.

PREFACE

This thesis was done in Microsoft Mobile Corporation in Tampere, Finland. I would like to thank Samuli Pietilä giving me this opportunity, and Jarno Luukkonen for providing the subject for the thesis. My thanks also belong to Jukka Hietaranta and Petri Ikonen for providing valuable insight, guidance and feedback. I would also like to thank the whole RF team for providing great working atmosphere and for their advice.

I am also very grateful to D.Sc. (Tech) Olli-Pekka Lunden and Professor Mikko Valkama for all the supervision and advice I was granted during the writing process. My final thanks belong to Saara Viinikainen, my friends, and my family for providing support throughout this work.

Tampere, 30.6.2015

Pasi Peijariniemi

TABLE OF CONTENTS

LIST OF FIGURES

ABBREVIATIONS AND SYMBOLS

3GPP	3rd Generation Partnership Project
ACLR	Adjacent Channel Leakage Power Ratio
CDMA	Code Division Multiple Access
DL	Downlink
DOE	Design of Experiment
ETSI	European Telecommunications Standards Institute
FDD	Frequency Domain Duplex
GSM	Global System for Mobile Communications
IC	Integrated Circuit
LTE	Long-Term Evolution
NF	Noise Figure
OFDMA	Orthogonal Frequency Division Multiple Access
PA	Power Amplifier
PCB	Printed Circuit Board
RB	Resource Block
RCT	Radio Communication Tester
RF	Radio Frequency
SC-FDMA	Single Carrier Frequency Division Multiple Access
SNR	Signal to Noise Ratio
S-parameters	Scattering Parameters
TDD	Time Domain Duplex
TEM	Transverse Mode
UL	Uplink
VNA	Vector Network Analyzer
WCDMA	Wideband Code Division Multiple Access

A	Voltage amplitude [V]
BW	Bandwidth [Hz]
a_0, a_1, a_2, a_3	Taylor series coefficients
c	Speed of light in a vacuum, $3.8 \cdot 10^8$ m/s
C’	Capacitance per unit length [F/m]
dB	Decibel
f	Frequency [Hz]
G’	Conductance per unit length [S/m]
K	Boltzmann’s constant, $1.38 \cdot 10^{-23}$ J/ °K
L	Length of the transmission line
L’	Inductance per unit length [H/m]
P	Power [W]
R’	Resistance per unit length [Ω/m]
V^-	Voltage wave moving from the system
V^+	Voltage wave moving to the system
v_i	Input voltage
v_o	Output voltage
v_p	Phase velocity [m/s]
Z	Impedance [Ω]
α	Attenuation constant [dB/m]
β	Phase constant [rad/m]

γ	Complex propagation constant
Γ	Voltage reflection coefficient
ϵ	Permittivity [F/m]
ϵ_o	Permittivity of free space [F/m]
ϵ_r	Relative permittivity, relative dielectric constant
λ	Wavelength [m]
μ	Permeability [H/m]
μ_o	Permeability of free space [H/m]
ω	Angular frequency [rad/s]

1. INTRODUCTION

Available time is one of the most important aspects of projects. In an ideal project infinite amount of time is had to make decisions and reach design goals. However, in many industrial projects the available time is highly limited. To be able to bring the product to market in a desired period of time, a certain time is available for each phase of the design and manufacturing process. In many cases this has created the need of new and faster methods to keep time tables. This holds true also in radio frequency (RF) design process, which may include, for example, simulation and matching network design.

In RF simulations the goal is to acquire component values for all the RF signal routes to ensure proper performance for the device. In addition to limited time, there is also limited physical available space on the printed wired board (PWB), meaning that only restricted amount of components can be used. In addition, transmission lines (conductors) have to also adapt to the limited space. The performance required for the device is described in specifications provided by the 3rd Generation Partnership Project (3GPP) [1].

What makes the matching network simulations time consuming is that there are multiple different technologies and frequencies (signal routes) in use. Almost all of them have unique key components and layout solutions. Currently most commercial mobile phones support at least two of the technologies available today: Global System for Mobile Communications (GSM), Code Division Multiple Access (CDMA), Wideband Code Division Multiple Access (WCDMA), Long-Term Evolution (LTE), or LTE Advanced. In addition, the number of usable bands is ever increasing and the time available for simulations remains the same. Therefore, there is demand for alternative methods that would achieve results faster without compromising accuracy.

At the moment, it is necessary to wait that the PWB layout is finished to be able to start simulating proper impedance matching component values. In this thesis, the focus is to find effects of chosen transmission lines when the length is varied within predetermined limits. If a limit is found where the effect is negligible, length of transmission lines could be determined to be within that limit. This would indicate the possibility to use any transmission line length within the limit in simulation model, and simulation process could be started before layout is entirely completed. Information might also prove useful if layout changes are required later in the design process to tell whether changed transmission line lengths have critical effect.

A tool called design of experiment (DOE) is used to test several limits. In DOE, input variables are chosen and their effect is studied on chosen outputs by varying the input

values. Usually DOE is used to find optimal values for inputs in order to optimize outputs. However, this thesis approaches DOE in different angle and aims to find out if it can be applied to define transmission line lengths within limits where no major variation is detected in performance parameters. In this thesis the study is performed on two LTE-FDD RF front ends using Agilent ADS as the simulation and analysis tool.

Chapter 2 gives a brief introduction to important theoretical areas necessary to understand this thesis, such as transmission line theory and scattering parameters. Chapter 3 describes the properties of the LTE and its electrical network under simulation. Chapter 4 defines what DOE is and how it is applied in this thesis. Chapters 5 and 6 present the simulation results for the simulated front ends, including short discussion regarding the results. Chapter 7 concludes this thesis with summary of the results and applicability of DOE in RF simulations.

2. RADIO FREQUENCY NETWORK THEORY

In this chapter the background theory that is necessary to understand this thesis is introduced. First section focuses on important aspects of transmission lines and briefly describes why the length of a conducting wire is necessary take into consideration during simulations. Second section introduces scattering parameters, a common parameters used in RF design, which describe the small signal behavior of a device. Third section briefly deals with noise and its importance, especially, in a receiver. Fourth section focuses on intermodulation distortion. Fifth section gives the basics with impedance matching using different approaches. Finally, the sixth section gives a brief introduction to the LTE technology.

2.1 Transmission line theory

Transmission line is a conductor where the electrical size becomes comparable to the wavelength [2, p. 49]. When the frequency is high enough voltages cannot be assumed to stay constant through the length of the conductor due to propagation delay, comparable to signal period. Whereas, if the frequency would be low enough the voltage could be assumed to be constant, which is the case in circuit theory [2, p. 49]. All conducting wires, usually having homogenous structure, can be analyzed as transmission lines. If electrical length is small compared to the wavelength, transmission line theory can be neglected to not make the circuit analysis unnecessary complex. However, in RF design conductors are generally considered as transmission lines.

To describe the voltage and current in the transmission line as a function of time and distance telegrapher's equations, a result from Maxwell's equations, were introduced in the late 19^{th} century [2, p. 55]. They are mostly used in RF but can be applied to, for example, power line design.

Transmission lines have always at least two conductors for transverse electric and magnetic mode (TEM) propagation, for example the ground plane and the signal line. Therefore, the transmission line is possible to model with distributed lumped element network [2, p. 49]. Illustration of infinitesimal piece of transmission line as a lumped element circuit is presented in Figure 1.

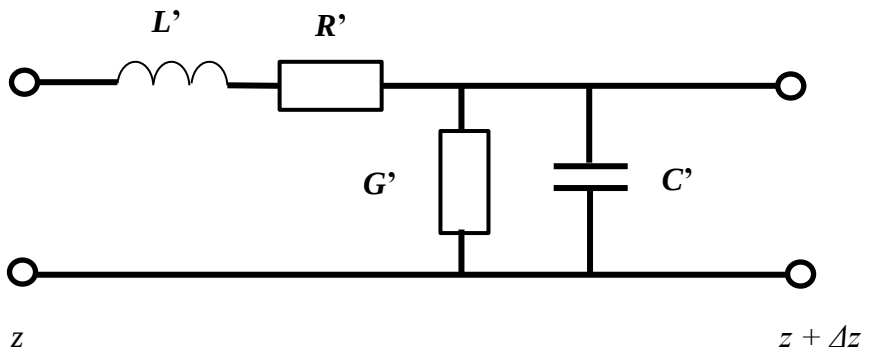

Figure 1. *Transmission line modeled as lumped-element circuit.*

The transmission line is divided into infinitesimal length of *Δz*, which has certain characteristics defined as follows: *R*' = series resistance per unit length (for both conductors), *L*' = series inductance per unit length (for both conductors), *C*' = shunt capacitance per unit length, and *G*' = shunt conductance per unit length. Respectively, v(*z*,*t*) and *i*(*z*,*t*) present the voltage and current on any point of the line at any given time.

Using Ohms and Kirchoff's voltage law the following equation can be applied for the circuit:

$$v(z,t) = R'\Delta z\, i(z,t) + L'\Delta z \frac{\partial i(z,t)}{\partial t} + v(z+\Delta z,t) \tag{1}$$

Both sides of Equation (1) is then divided with Δz and some rearranging is performed.

$$\frac{v(z+\Delta z,t) - v(z,t)}{\Delta z} = -R'\, i(z,t) - L' \frac{\partial i(z,t)}{\partial t} \tag{2}$$

Since we are inspecting an infinitesimal part of the transmission line, the value of Δz approaches zero (Δz →0). Therefore, the left side of Equation (2) can be expressed as derivative:

$$\frac{\partial v(z,t)}{\partial z} = -R'\, i(z,t) - L' \frac{\partial i(z,t)}{\partial t} \tag{3}$$

Kirchoff's current law can also be applied for the circuit presented in Figure 1:

$$i(z,t) = C'\Delta z \frac{\partial v(z+\Delta z,t)}{\partial t} + G'\Delta z\, v(z+\Delta z,t) + i(z+\Delta z,t) \tag{4}$$

With Equation (4) the same operations as with Equation (1) are performed: division with *Δz* and rearranging.

$$\frac{i(z+\Delta z,t)-i(z,t)}{\Delta z}=-C'\frac{\partial v(z+\Delta z,t)}{\partial t}-G'\,v(z+\Delta z,t) \tag{5}$$

Once again, it can be noted that when *Δz* approaches zero (*Δz* → 0) the Equation (5) can be presented in derivative form.

$$\frac{\partial i(z,t)}{\partial z}=-C'\frac{\partial v(z,t)}{\partial t}-G'\,v(z,t) \tag{6}$$

For sinusoidal steady state condition Equation (3) and (6) can be simplified to:

$$\frac{dV(z)}{dz}=\ -(R+j\omega L)I(z) \tag{7}$$

and

$$\frac{dI(z)}{dz}=\ -(G+j\omega C)V(z) \tag{8}$$

Equations (7) and (8) can be simultaneously solved to receive wave equations for voltage *V*(*z*) and current *I*(*z*):

$$\frac{d^2V(z)}{dz^2}=\gamma^2V(z) \tag{9}$$

$$\frac{d^2I(z)}{dz^2}=\gamma^2I(z) \tag{10}$$

The complex propagation constant γ is defined in Equation 11.

$$\gamma=\alpha+j\beta=\sqrt{(R+j\omega L)(G+j\omega C)} \tag{11}$$

Where, α is the attenuation constant and β the phase constant. On the lossless case *R*=*G*=0, in this case $\gamma=j\omega\sqrt{LC}$ → α = 0, and $\beta=\omega\sqrt{LC}$.

Travelling wave solutions for lossless case are presented in the following equations.

$$V(z)=V^+e^{-j\beta z}+V^-e^{j\beta z} \tag{12}$$

$$I(z)=I^+e^{-j\beta z}-I^-e^{j\beta z} \tag{13}$$

The term $e^{-\beta z}$ and $e^{\beta z}$ represent the wave propagation to +*z* and –*z* direction respectively. Therefore, the total voltage is consisted of incident and reflected waves. Characteristic impedance Z_0 of the line can then be defined as

$$Z_0 = \frac{V^+}{I^+} = \frac{V^-}{I^-} \tag{14}$$

Characteristic impedance can defined using the lumped element circuit illustrated in Figure 1. The lumped model is applied infinite amount of times in the real length of the transmission line. The general definition for characteristic impedance is then as follows:

$$Z_0 = \sqrt{\frac{R' + j\omega L}{G' + j\omega C}} \tag{15}$$

Equation (14) can then be modified to be represented according to voltages:

$$I(z) = \frac{V^+}{Z_0} e^{-j\beta z} - \frac{V^-}{Z_0} e^{j\beta z} \tag{16}$$

The relation between incident and reflecting wave can be used to define the relation between the characteristic impedance of the transmission line (Z_0) and the impedance of the load (Z_l) connected to the transmission line. Reflection coefficient Γ can then be defined as:

$$\Gamma = \frac{V^-}{V^+} = \frac{Z_l - Z_0}{Z_l + Z_0} \tag{17}$$

Figure 2 illustrates a lossless transmission line with a connected load.

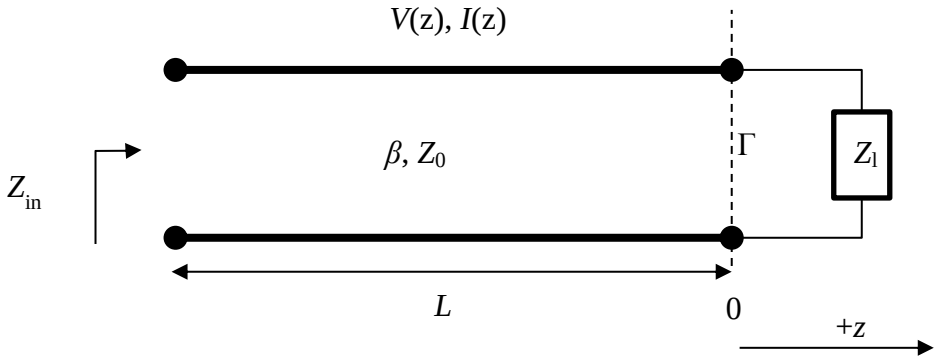

Figure 2. *Transmission line with a connected load.*

Using the relation between incident and reflected waves, the input impedance of the transmission line with connected load can be determined. Input impedance at distance L from the load can be defined as:

$$\mathrm{Z_{in}} = \frac{V(-L)}{I(-L)} = \frac{V^+ e^{j\beta L} + V^- e^{-j\beta L}}{V^+ e^{j\beta L} - V^- e^{-j\beta L}} Z_0 \tag{18}$$

Input impedance can also be represented using characteristic impedance of the line and impedance of the load if Equation (17) is applied to Equation (22).

$$\mathrm{Z_{in}} = Z_0 \frac{Z_l + jZ_0 \tan \beta L}{Z_0 + jZ_l \tan \beta L} \tag{19}$$

Therefore, we can determine that the input impedance is depended on the length of the transmission line if $Z_0 \neq Z_l$. [2, pp. 57-60]

There are multiple different types of transmission lines. The most relevant to this thesis are microstrip and stripline types of transmission lines. The two mentioned transmission line types are illustrated in Figure 3.

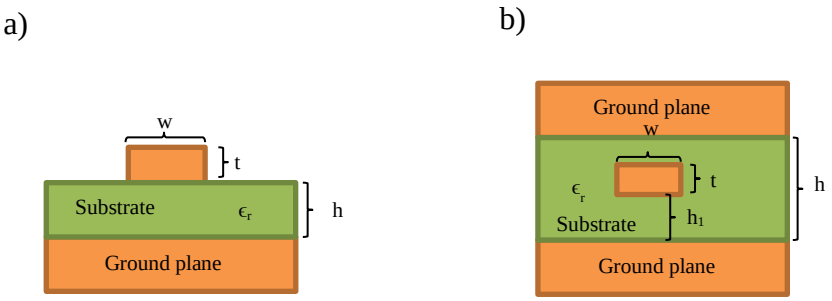

Figure 3. *A side view of a) a microstrip and b) a stripline transmission line.*

Microstrip is a transmission line that is fabricated above a ground plane with a substrate between them [2, p. 143]. Stripline is positioned inside between two ground planes with substrate [2, p. 137]. Note that it does not have to be positioned in the middle of the ground planes. Transmission line has the thickness of *t* and width of *w*. Substrate has the relative dielectric constant of ϵ_r and has the height of *h*. All of these parameters have an effect to the characteristic impedance of a transmission line [2, pp. 139-145]. Microstrip lines are typically used on top of or bottom of a printed wired board, whereas striplines are used in multilayer boards in the middle layers.

2.2 Scattering Parameters

In electronics it is required to be able to describe linear electrical networks with a set of parameters. Of course, there are many kinds of parameters existing. For example, impedance (Z-) or admittance (Y-) parameters. However, these set of parameters depend on open and short circuits. In case of high frequency it may become complicated to have a real short or open circuit due to parasitic components when measuring the circuit. The solution to the problem is scattering parameters, or S-parameters [2, p. 174].

Instead of open or short circuit methods S-parameters rely on reference impedances. Each port is connected to a reference impedance, which in most situations is 50 Ω. However, it is entirely possible that the matching impedance could be different than 50 Ω, and it could also be different for each port. From each port of the network under investigation, the incident and reflecting voltage waves are measured. Each port represents a possible input and output route for the network. Therefore, an N-port network can be represented with N^2 set of S-parameters. [2, pp. 174-175] Figure 4 illustrates the general situation in the case of N-port system.

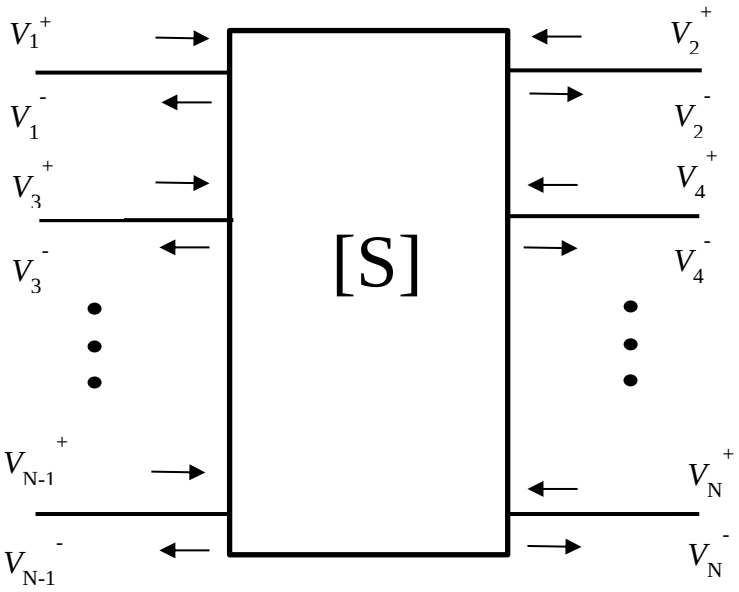

Figure 4. *N-port system.*

Where V^+ is the incident and V^- the reflected wave.

In addition, S-parameters can be converted to Z-, Y-, H-, or ABCD-parameters, and vice versa [2, p. 174].

S-parameters are defined with incident and reflected voltage waves. In case of an N-port system, as illustrated in Figure 4, the following matrix is formed.

$$\begin{bmatrix} V_1^- \\ V_2^- \\ \vdots \\ V_N^- \end{bmatrix} = \begin{bmatrix} S_{11} & S_{12} & \cdots & S_{1N} \\ S_{21} & \ddots & & S_{2N} \\ \vdots & & \ddots & \vdots \\ S_{N1} & S_{N2} & \cdots & S_{NN} \end{bmatrix} \begin{bmatrix} V_1^+ \\ V_2^+ \\ \vdots \\ V_N^+ \end{bmatrix} \tag{20}$$

Matrix presented in Equation (20) can also be expressed in a simpler form.

$$[V^-] = [S][V^+] \tag{21}$$

It is also desirable to determine a specific element from the matrix.

$$S_{ij} = \frac{V_i^-}{V_j^+}\Bigg| V_k^+ = 0, k \neq j \tag{22}$$

In words, Equation (22) means that a single element in the s-matrix is determined using only a single port as an input and another as an output. The only input signal comes from port *j*, and port *i* is the output port. [2, pp. 174-175] For example, S_{21} would tell what kind of output is caused in port 2 by the input in port 1, in other words insertion loss or gain from one port to another. As another example, S_{11} would define how much power would be reflected back to the port 1, which is used as an input. Therefore, S_{11} is very useful to study impedance matching of a network.

S-parameters can be obtained from the manufacturer, and in turn the acquired S-parameters can be used in simulations to determine, for example, the proper matching circuit for an electronic network. It is also possible to measure them if vector network analyzer (VNA) is available. In some cases, the models for different components in a circuit are so well known that accurate S-parameters can be achieved by simulating [2, p. 174].

2.3 Noise

Noise happens due to random motion of charges and charge carriers which, in turn, will cause random fluctuations in voltage. Noise can be caused by external systems or internally generated in the device. [2, p. 487] By default noise is present in all electronic systems [3, p. 37]. Especially in communication technology the noise will determine the minimum signal level the receiver is able to detect, which is why it is important to match the receiver accordingly to maximize the signal to noise ratio (SNR).

The random motion of the electronics, the noise, is caused by a number of reasons. The most common type of noise is thermal noise, which is present in all systems where temperature is above absolute zero [2, p. 489]. Thermal noise is caused by thermal vibrations of bound charges [2, p. 488].

There are also other types of noise such as shot noise and flicker noise [2, p. 488]. Both can be caused by solid-state devices, which are heavily used in integrated circuits (IC) [4]. Therefore, they are also present in communication systems, such as mobile phones.

Noise is particularly important in receiver circuits. The first amplifying stage in the receiver has the most impact to the overall noise performance of the system. Therefore, we want to minimize the amount of noise amplified. Noise figure (NF) of the device describes how much the SNR degrades in the system. Noise figure is defined as the ratio of SNR in the input to the SNR in the output in decibels.

$$NF = 10log\frac{SNR_{in}}{SNR_{out}}\ dB \tag{23}$$

The input noise power is assumed to be the noise power from a matched resistor at T_0 = 290 K. Using Planck's black box radiation law and Rayleigh-Jeans approximation, the input noise power can be defined as:

$$P_{noise,in} = kT_0BW \tag{24}$$

where k is the Boltzmann's constant ($1.38 \cdot 10^{-23}$ J/ °K) and BW the bandwidth of the system (Hz). Output noise is the sum of amplified input noise and the noise generated in the system. [2, pp. 489-494] Noise figure can often be minimized with impedance matching [2, pp. 557-559].

2.4 Intermodulation distortion

Every practical electrical component is not totally linear, where output would be directly proportional to input(s) [3, p. 11]. With very low power levels noise will be the limiting factor whereas with high power levels the device might become broken. Often, the area where the device works linearly enough is called the dynamic range of the device [2, p. 505].

The output of a nonlinear device can be described with Taylor series [2, p. 501]:

$$v_o = a_o + a_1v_i + a_2v_i^2 + a_3v_i^3 + \cdots \tag{25}$$

Where v_o is the output voltage, v_i the input voltage, and a_0, a_1, a_2, and a_3 are the Taylor coefficients.

Usually the output will have more than one non-zero coefficient. Assuming that input would be single frequency sinusoidal signal $v_i = A\sin(\omega_0 t)$ Taylor series would indicate that there are more than one frequency component in the output. In other words, multiples (ω_0, $2\omega_0$, $3\omega_{0\ \ldots}$) of the input signal frequency will be generated at the output [2, p. 502]. Multiples, in turn, are commonly known as harmonics of the fundamental signal.

However, when considering a system where there are more than one frequency in the input the situation can be very different. For example, if the input would have two frequencies with equal amplitudes $v_i = A[\sin(\omega_1 t)+\sin(\omega_2 t)]$, it could be seen from the Taylor series that the output would be consisted of not just harmonics of both frequencies but also from intermodulation products [2, pp. 502-503]. Intermodulation products are the formed from the sums and subtractions of the input frequencies and their multiples. Figure 5 gives the illustration of several generated intermodulation output products [2, p. 504].

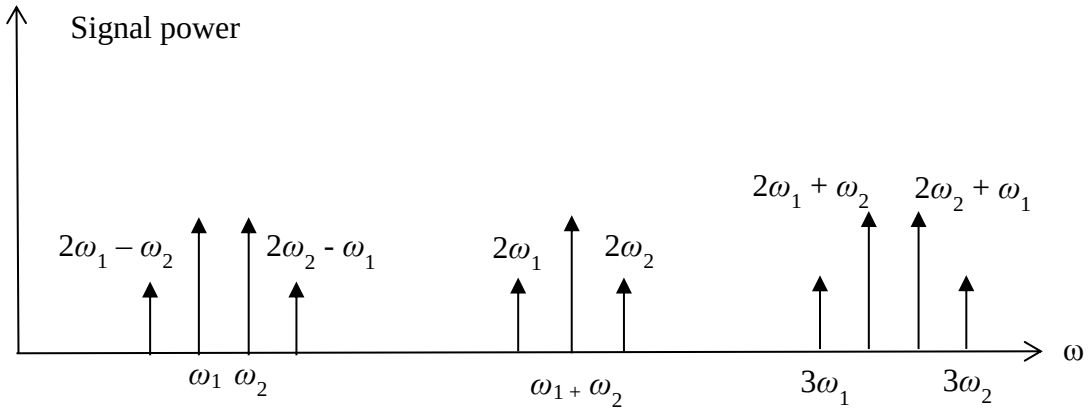

Figure 5. *Output frequencies of a nonlinear system with two input frequencies ω_1 and ω_2.*

With non-linear behavior two frequency input will generate multiple intermodulation products. Modern communication technologies may include a greater number of carriers or subcarriers in the transmission. In nonlinear behavior this will lead to an even greater number of intermodulation products that may cause problems, such as power spreading to adjacent channels in a cellular system. [5, p. 27] [6, pp. 184-186] For example, in telecommunication applications the transmitted signal consists from a number of carriers or subcarriers that cause intermodulation products [6, pp. 251-255]. These intermodulation products cause power spreading to adjacent channels, which is important to minimize so that specifications are met. [6, pp. 19-21]

2.5 Impedance matching theory

Impedance matching, in practice, means that a certain impedance is transformed to another. Usually the goal is to maximize power transfer. However, this is not always the case and sometimes mismatch is even desired. For example, in a situation where a specific gain is desired or the noise needs to be minimized the maximum power transfer may not be the ideal [2, p. 553].

Transformation, or impedance matching, can be done different ways. However, not all methods are reasonable in every case. For example, matching can be done with resistors. Naturally that attenuates the signal and, thus, is not suitable in situations where signal attenuation in the matching network is not desirable. Matching can also be attained with other lumped element components: capacitor and inductor. Ideally capacitors and inductors are lossless components. Though, in practice, some power will be lost in these components, too.

Impedance matching could also be done with many other ways from transmission line to active device based impedance matching [2] [7]. However, usually in mobile device design lumped element components are chosen due to the size limits and the wavelength

of the signal. For example, adding stubb lines (transmission line matching method) can take a lot of space, and is thus not usually a valid option.

One of the most common applications of impedance matching is to match the source and load impedances so that maximum power can be delivered from source to load. This is commonly known as conjugate matching. [6, pp. 12-13] Figure 6 illustrates a situation where a source, a generator with internal impedance (Z_g), is connected to a load impedance (Z_l).

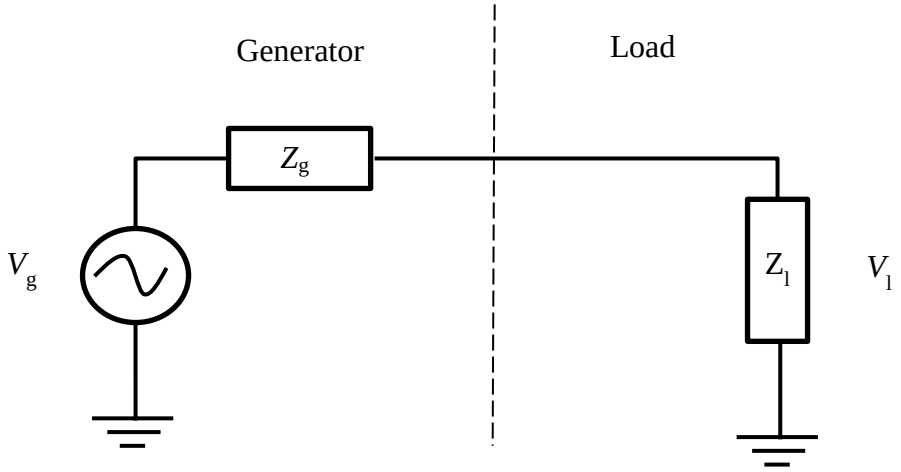

Figure 6. *Generator with internal impedance Zg and load impedance Zl.*

To determine the impedance values for both source and load for maximum power transfer a simple analysis can be performed. According to Ohm's law the power in the load is described in Equation (26).

$$P_l = Re\{V_l I^*\} = Re\left\{\left(V_g \frac{Z_l}{Z_g + Z_l}\right)\left(\frac{V_g}{Z_g + Z_l}\right)^*\right\} = |V_g|^2 \frac{Re\{Z_l\}}{|Z_g + Z_l|^2} \tag{26}$$

where V_l is the peak voltage of the load, V_g the peak voltage of the generator, I the current, Z_g the complex generator impedance $R_g + X_g$, and Z_l the complex load impedance $R_l + X_l$. Equation (26) can then be rewritten as:

$$P_l = |V_g|^2 \frac{R_l}{(R_l + R_g)^2 + (X_l + X_g)^2} \tag{27}$$

Assuming that the generator impedance is fixed we can then differentiate Equation (27) with respect to R_l and X_l to find which values yield the maximum power transferring. The results of the analysis will be that $R_l = R_g$ and $X_l = -X_g$. Therefore, it can be expressed that in conjugate matching $Z_l = Z_g^*$. [2, p. 79] As mentioned in section 2.1, if

there is a transmission line, the impedance to be matched will change as a function of length of the transmission line. Therefore, transmission lines will also have an effect to the desired matching components.

However, sometimes it is not reasonable to apply conjugate matching. In receiver circuits, for example, another important issue is noise and usually the receiver is matched towards optimum noise source to improve noise figure of the circuit [2, p. 222]. This means that the load is matched so that the noise figure of the device is as small as possible, in other words, the SNR is optimized. Conjugate matching might not be viable option in the transmitter side either. As the power amplifier may behave as nonlinear device there may be power spread to adjacent channels. Therefore, matching nonlinear devices in practice requires finding the optimal load or source, which may be different from the complex conjugate impedance.

3. OVERVIEW OF LTE TECHNOLOGY

In the beginning of 2010 most mobile phones supported only 2G and 3G connections, even though the LTE technology was standardized as early as 2008 [8]. Today, however, many cellular phones already support LTE which is commonly marketed as 4G connection [9]. 4G offers significant upgrades from 3G, such as increased uplink (UL) and downlink (DL) speeds in addition to decreased latency [10].

One of the main features of LTE is the change from previous access technology CDMA to orthogonal frequency division multiple access (OFDMA) in the downlink and single carrier FDMA (SC-FDMA) in the uplink. OFDMA uses a number of closely spaced modulated subcarriers that can overlap each other. However, they will not interfere with each other as the carrier spacing is equal to the reciprocal of the symbol period. [11] Therefore, it is possible to make more efficient use of the available bandwidth (BW) when compared to previous methods, potentially meaning more network capacity [12] [10]. SC-FDMA is also a form of OFDMA but it is modified so that it fits the mobile devices: while OFDMA has high peak to average power ratio, SC-FDMA has low peak to average power ratio which makes it more user friendly in terms of power consumption [13].

LTE can be divided in two duplexing schemes: frequency domain duplexing (FDD) and time domain duplexing (TDD). Duplexing scheme defines in which way transmitting and receiving is handled. Main difference is that FDD uses separate frequencies for DL and UL, while TDD uses different time slots for transmitting and receiving on the same frequency. [14] Both of the duplexing schemes are widely used.

Figure 7 illustrates a typical LTE-FDD and LTE-TDD front end block diagrams. It can be noted that the main difference is how transmitter and receiver are located in different duplexing schemes. In FDD, the duplexer separates the transmitting and receiving sides from each other. In TDD transmitter and receiver are located in the same IC, where an internal switch determines whether it is transmitting or receiving. [3, pp. 103-104]

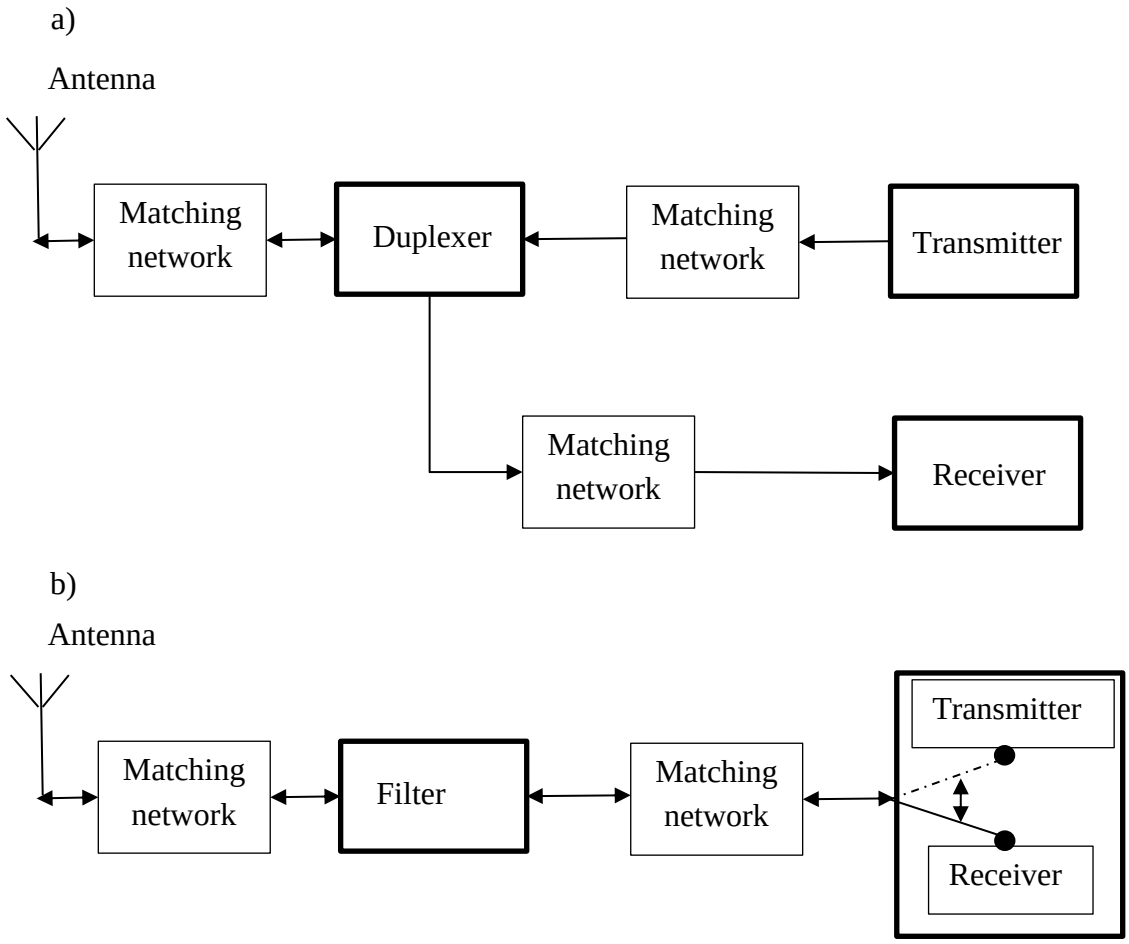

Figure 7. *RF Block diagram of a typical a) LTE-FDD b) LTE-TDD front end.*

LTE channels can utilize different bandwidths. Each channel bandwidth is further divided in resource blocks (RB). Table 1 describes all possible channel bandwidths and the corresponding maximum number of RBs. Each RB is consisted of 12 subcarriers spaced 15 kHz apart. Therefore, as the channel bandwidth increases and number of RBs in use increases, so does the channel capacity. [13]

As LTE uses multiple carriers there will also be intermodulation distortion included. This has to be taken into account when designing RF devices, such as mobile phones. One way to study the intermodulation distortion in mobile device design is to measure the power that spreads to the adjacent channel, also known as adjacent channel leakage ratio (ACLR). [5, p. 27] ACLR is defined as the ratio of transmitted power to the power in the adjacent radio channel.

Table 1. *Maximum number of resource blocks corresponding to channel bandwidth.*

Channel Bandwidth (MHz)	**Maximum # of RBs**
1.4	6
3	15
5	25
10	50
15	75
20	100

4. DESIGN OF EXPERIMENT

Design of experiment is an experimental way to find how different input factors impact the output response. In other words, a series of experiments are run while changing the input(s) between each experiment. Typically, DOE is used as a tool to optimize outputs. In addition, it is also possible to find critical components with it. [15] DOE can be used in many applications, for example, in cooking amount of sugar could be one factor and taste of the cooked product the output response. DOE can also be utilized in RF design. [16] [17]

Before DOE analysis can be started, three items need to be identified: input factors, how input factors are varied, and outputs. Input factors can be, for example, varied with different limits. It is also possible to use different materials as input, too [18]. As an example, in cooking natural sugar could be replaced with synthetic sugar. Outputs are the responses where input factors are expected to have an impact.

In some cases, it is possible that there are a lot of input factor candidates. In a situation like this an operation called screening can be performed. In screening process, all the critical components are identified. Identifying is done by conducting a fixed amount of DOE. When the critical components are identified, further DOE analysis can be done using those factors. [19]

To identify the critical factors the gathered data needs to be analyzed. For example, main effect for each variable can prove very useful. Main effect is calculated by as the average response at the two levels for a given factor [17]. Another way to present the data is a Pareto diagram, which shows the percentage of each factors contribution to variation. Through DOE it is also possible to study the effects, or interaction, of two or more combinations. In some cases this can be used to determine the optimal values for certain inputs. [15]

4.1 Design of Experiment in ADS

In this thesis the RF simulation work is performed using Agilent Advanced Design system (ADS). Version used to in this thesis is ADS 2012.08. The tool contains required tools to perform both RF simulations and DOE analysis. [15]

ADS contains also another tool, in addition to DOE, that could be used to do different tolerance and sensitivity analysis: Monte Carlo (MC) simulation. In MC, the input factor values are varied randomly according to predetermined probability function [20]

[21]. Typically MC is applied in yield simulations where the robustness of the design is studied. Randomization is also the main difference when compared to DOE, where different input factor value combinations are systematically applied.

DOE in ADS can be conducted in several different ways. Two first options are to use either full factorial (2-level) experiment or fractionalized factorial experiment. In full factorial experiment, input factors are changed according to their minimum and maximum values and all combinations are simulated. In fractionalized experiment a subset of full factorial experiment is run. Another option is to use Plackett-Burman experiment, which allows to do DOE in a user defined (multiple of four) number of runs making it useful, for example, for screening. [15]

Several options are also presented for multilevel designs. Multilevel design indicates that each factor may have more than two levels that are included in the DOE analysis. For example, 3-level full factorial analysis is otherwise the same as the 2-level factorial experiment but also the nominal points are taken in to the analysis. [15]

MC method is not a viable option as the values are chosen randomly. Therefore, additional amount of simulation runs would be needed in order to verify that all combinations of transmission line lengths are simulated. MC would also produce a lot of information that would not be useful, or may be a duplicate of already simulated information. However, this can be avoided reliably using DOE. Therefore, 2-level full factorial DOE is chosen to be used in this thesis. Since only several input factors are determined the amount of data remains feasible, and there is no need to reduce the amount of experiments run. Full factorial analysis also provides the information of the worst case scenario.

4.2 DOE simulation setup for transmission lines

Design of experiment is applied to two different LTE-FDD front ends. LTE-FDD 1.9-GHz (band 2) and 700-MHz (band 12) bands are chosen. Chosen bands differ in components used, and in operation frequencies. Research is started using models that are built from an existing layout. Actual transmission line lengths are used as the nominal lengths, and DOE analysis is performed by varying the length from nominal lengths.

DOE is performed on 6 frequencies of interest in each band. The frequencies of interest are chosen to be UL and DL low, middle, and high channel frequencies. Low channel and high channel frequencies are chosen using 5 MHz channel bandwidth. Middle channel frequency stays the same with all channel bandwidths. All frequencies of interest are gathered in Table 2 [22].

Table 2. *List of channels and frequencies of interest.*

LTE band		Downlink			Uplink		
		Low	Middle	High	Low	Middle	High
2	Channel #	625	900	1175	18625	18900	19175
	Frequency (MHz)	1932.5	1960	1987.5	1852.5	1880	1907.5
12	Channel #	5035	5095	5155	23035	23095	23155
	Frequency (MHz)	731.5	737.5	743.5	701.5	707.5	713.5

For each front end network under investigation three transmission lines, which length may greatly vary depending on layout solutions, are included in the analysis. Figure 8 illustrates the RF front end in a simplified manner to show the location of the transmission lines under investigation. Position of the transmission lines in the block diagram is identical in both studied front ends. The lengths of the chosen transmission lines are defined as input factors. Their impact to return loss in transmitter (S_{11}), receiver (S_{22}), and antenna are studied in addition to the insertion loss in downlink and uplink paths.

Using port numbers illustrated in Figure 8, studied parameters can be defined with S-parameters. Therefore, transmitter return loss, antenna return loss and receiver return loss are defined as S_{11}, S_{22}, and S_{33} respectively. Uplink insertion loss and downlink insertion loss are defined as S_{21} and S_{32}.

It is decided that three different limits are analyzed. Limits are chosen to be ±50%, ±25%, and ±10% from nominal lengths. A full factorial (2-level) DOE analysis is performed with all investigated limits in Agilent Advanced Design System (ADS). This means that 2^x simulation results are acquired, where x is the number of input factors. In this case three input factors are chosen meaning eight simulations for each limit.

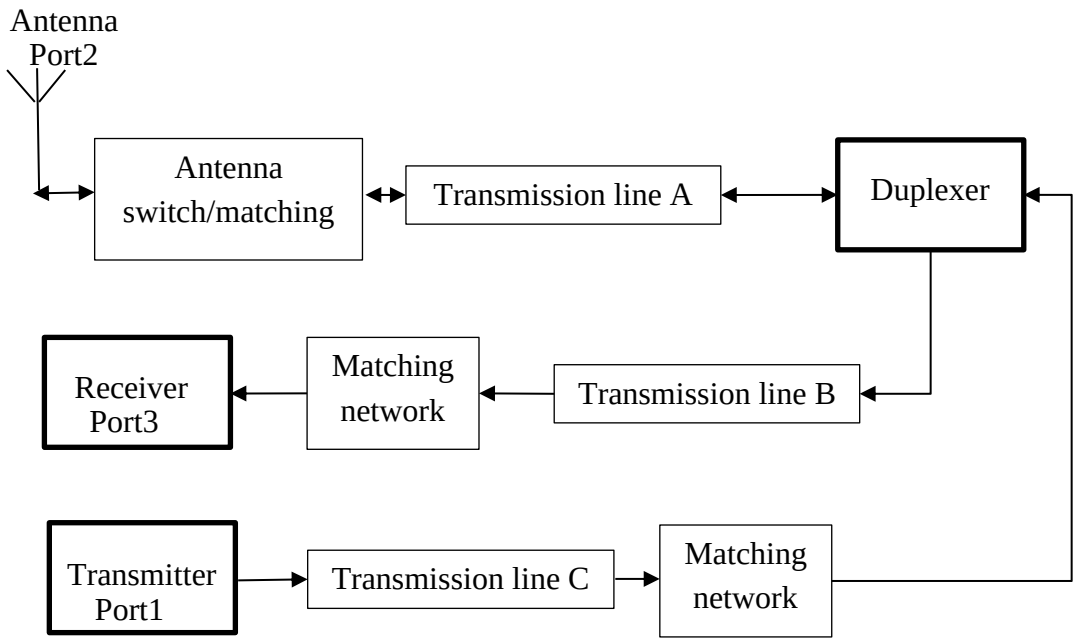

Figure 8. *RF LTE-FDD front end block diagram with the studied transmission lines included.*

5. 1.9-GHZ BAND 2 DOE ANALYSIS

For LTE band 2 transmission lines for DOE analysis are chosen as described in Figure 8. The transmission line lengths with different limit cases are gathered in Table 3.

Table 3. *LTE band 2 transmission line lengths for DOE analysis.*

Transmission line	Nominal (mm)	50% (mm)	-50% (mm)	25% (mm)	-25% (mm)	10% (mm)	-10% (mm)
ANT (A)	4.285	6.428	2.143	5.356	3.214	4.714	3.857
RX (B)	16.410	24.615	8.205	20.513	12.308	18.051	14.769
TX (C)	1.897	2.846	0.949	2.371	1.423	2.087	1.707

It can be noted that transmission line B is the longest transmission line in band 2 investigation. The nominal case will also be simulated so the variation in each different limit case can be compared to it.

5.1 Transmitter return loss

Next the return loss of the transmitter is studied. The return loss is calculated with reference to the transmitter load impedance that provides the optimized adjacent channel leakage ratio (ACLR) behavior. Only uplink frequencies are studied in this case. Figure 9 illustrates the simulated port in a block diagram.

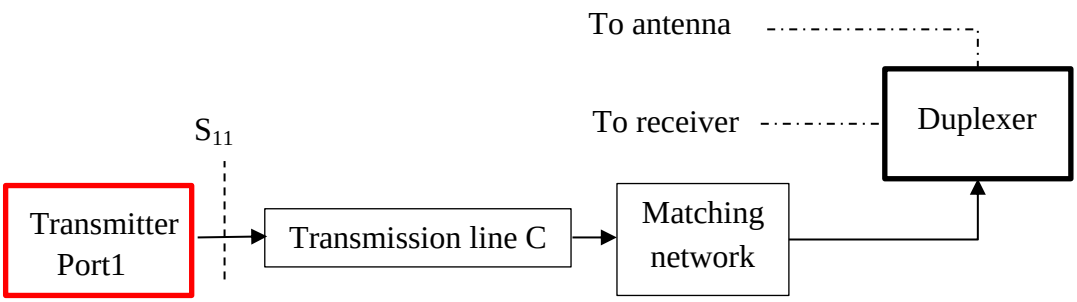

Figure 9. *Transmitter return loss is measured from port 1.*

Figure 10 shows the variation on studied frequency points when the length of transmission line is varied with different limits.

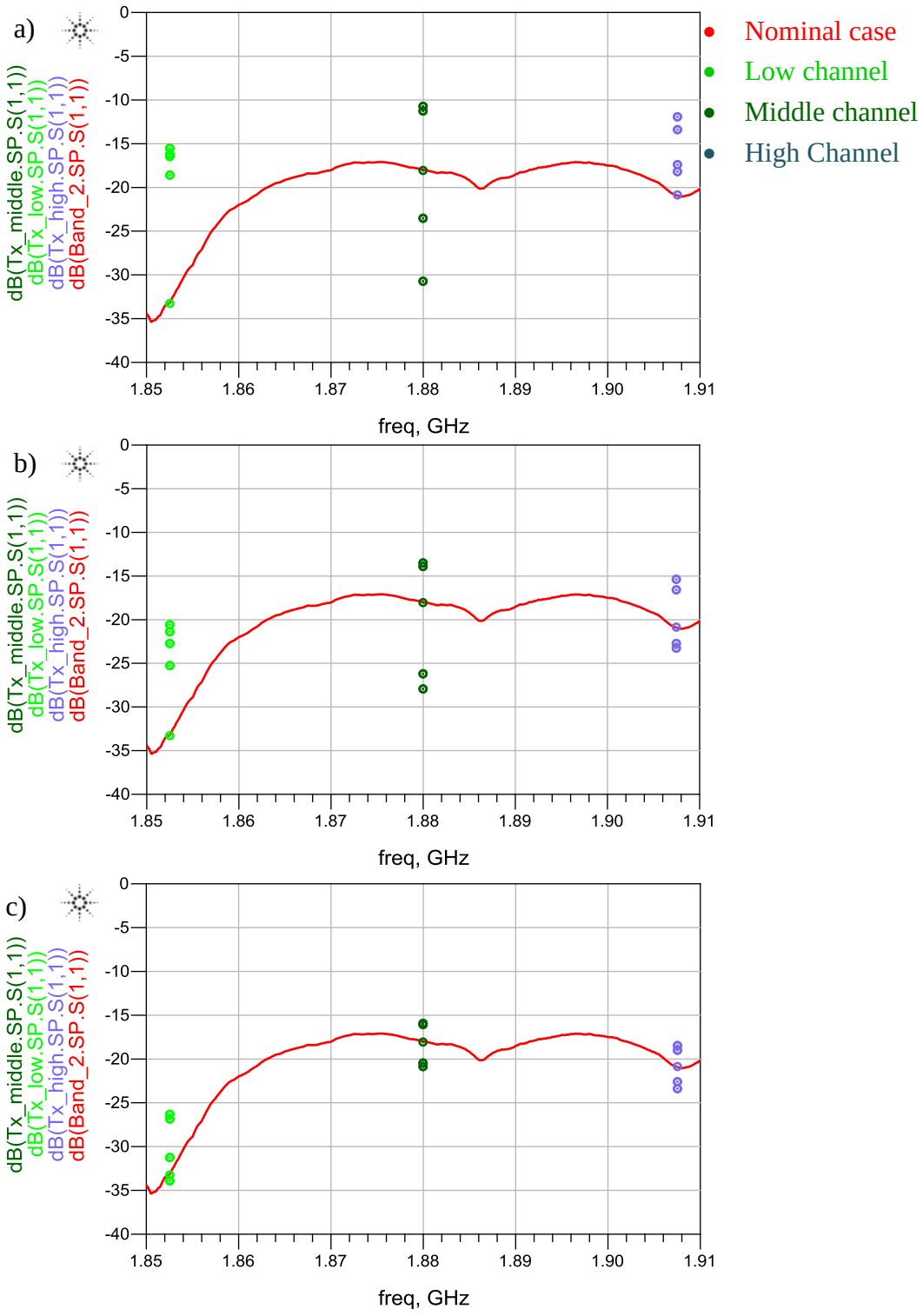

Figure 10. *LTE band 2 transmitter return loss with a) ± 50%, b) ± 25 %, and c) ± 10 % variation in transmission line lengths.*

Variation decreases on studied frequency points when limits are changed from ±50 % to ± 10 %. Different variations from nominal results are gathered in Table 4. -Δ shows the maximum variation to the negative direction, and +Δ shows the maximum variation to positive direction. If there is – sign, it shows that there is no variation to that direction.

Table 4. *Maximum variations in transmitter return loss from nominal case with different limit cases for LTE band 2.*

		± 50 %		**± 25 %**		**± 10 %**	
	Nominal (dB)	-Δ (dB)	+Δ (dB)	-Δ (dB)	+Δ (dB)	-Δ (dB)	+Δ (dB)
Low Channel	-33.262	-	17.775	-	12.735	0.694	6.935
Middle Channel	-18.005	22.309	7.245	9.922	4.515	2.865	2.134
High Channel	-20.898	-	9.007	2.334	5.519	2.422	2.501

Simulations showed that transmission line B has no effect on transmitter return loss. This applied to all simulated limit cases. It was also found that transmission line A has the most effect on the transmitter return loss on all limits and studied frequency points.

5.2 Antenna return loss

Antenna return loss is studied next. Figure 11 illustrates the simulated port in a block diagram.

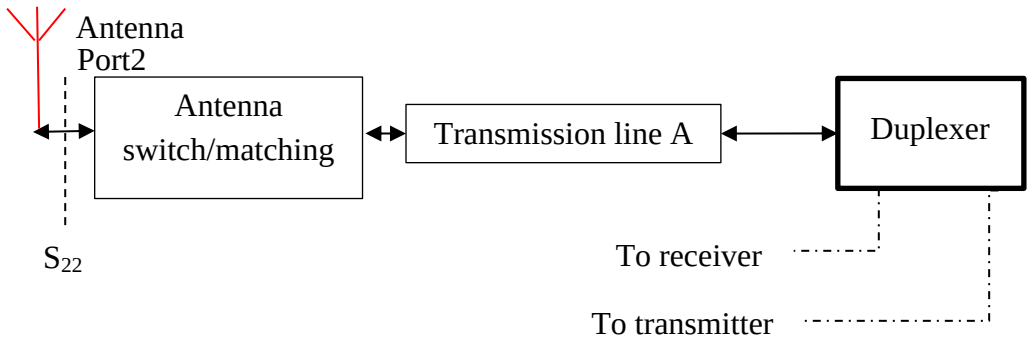

Figure 11. *Antenna return loss is measured from port 2.*

Figure 12 shows the variation in antenna return loss with different DOE limits. Both uplink and downlink frequencies are studied.

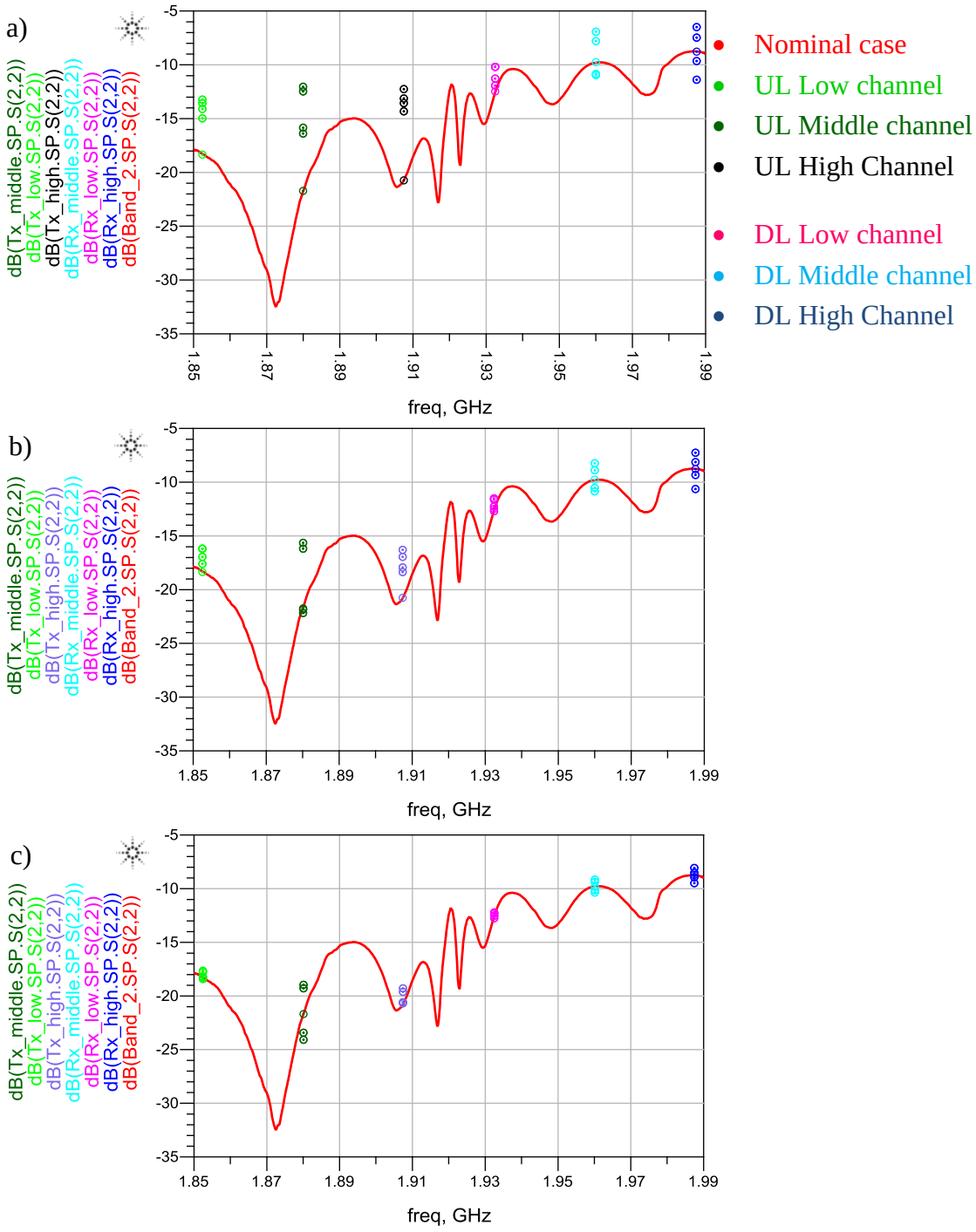

Figure 12. *Antenna return loss for LTE band 2 with a) ± 50 %, b) ± 25 %, and c) ± 10 % variation in transmission line lengths.*

Variation from nominal results decreases as the transmission line lengths are approaching the nominal length. Variation is higher on uplink frequencies than on downlink frequencies. Different variations from nominal results are gathered in Table 5. -Δ shows the maximum variation to negative direction, and +Δ shows the maximum variation to positive direction. If there is – sign, it shows that there is no variation to that direction.

Table 5. *Antenna return loss variation with different limits for LTE band 2.*

			± 50 %		**± 25 %**		**± 10 %**	
		Nominal (dB)	-Δ (dB)	+Δ (dB)	-Δ (dB)	+Δ (dB)	-Δ (dB)	+Δ (dB)
Uplink	Low Channel	-18.314	-	4.429	-	2.117	0.110	0.624
	Middle Channel	-21.719	-	9.684	0.137	6.039	2.321	3.119
	High Channel	-20.729	-	7.621	-	4.438	-	1.441
Downlink	Low Channel	-12.525	-	2.334	0.153	0.970	0.178	0.314
	Middle Channel	-9.803	1.148	2.631	1.077	1.579	0.555	0.632
	High Channel	-8.760	2.632	2.113	1.864	1.470	0.751	0.668

For uplink and downlink frequencies both, it was seen that transmission line A has the most contribution on antenna return loss variation. Transmission line B has no effect on uplink frequencies and transmission line C has no effect downlink frequencies.

5.3 Receiver return loss

In downlink return loss refers to the source impedance that provides the optimized receiver noise figure. Figure 13 shows the simulated port in the front end block diagram.

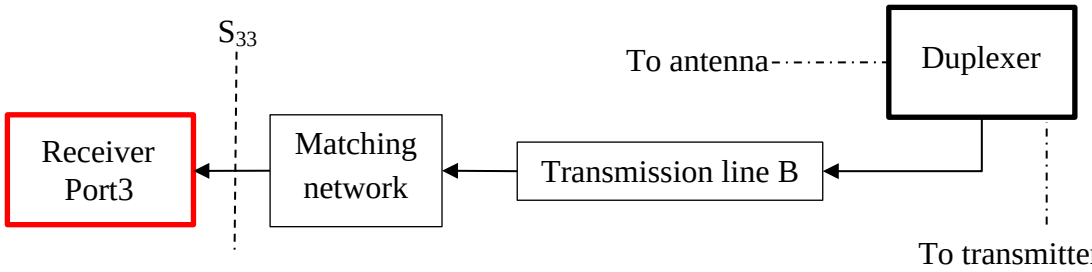

Figure 13. *Receiver return loss is measured from port 3.*

Figure 14 shows the variation in downlink low, middle, and high channels.

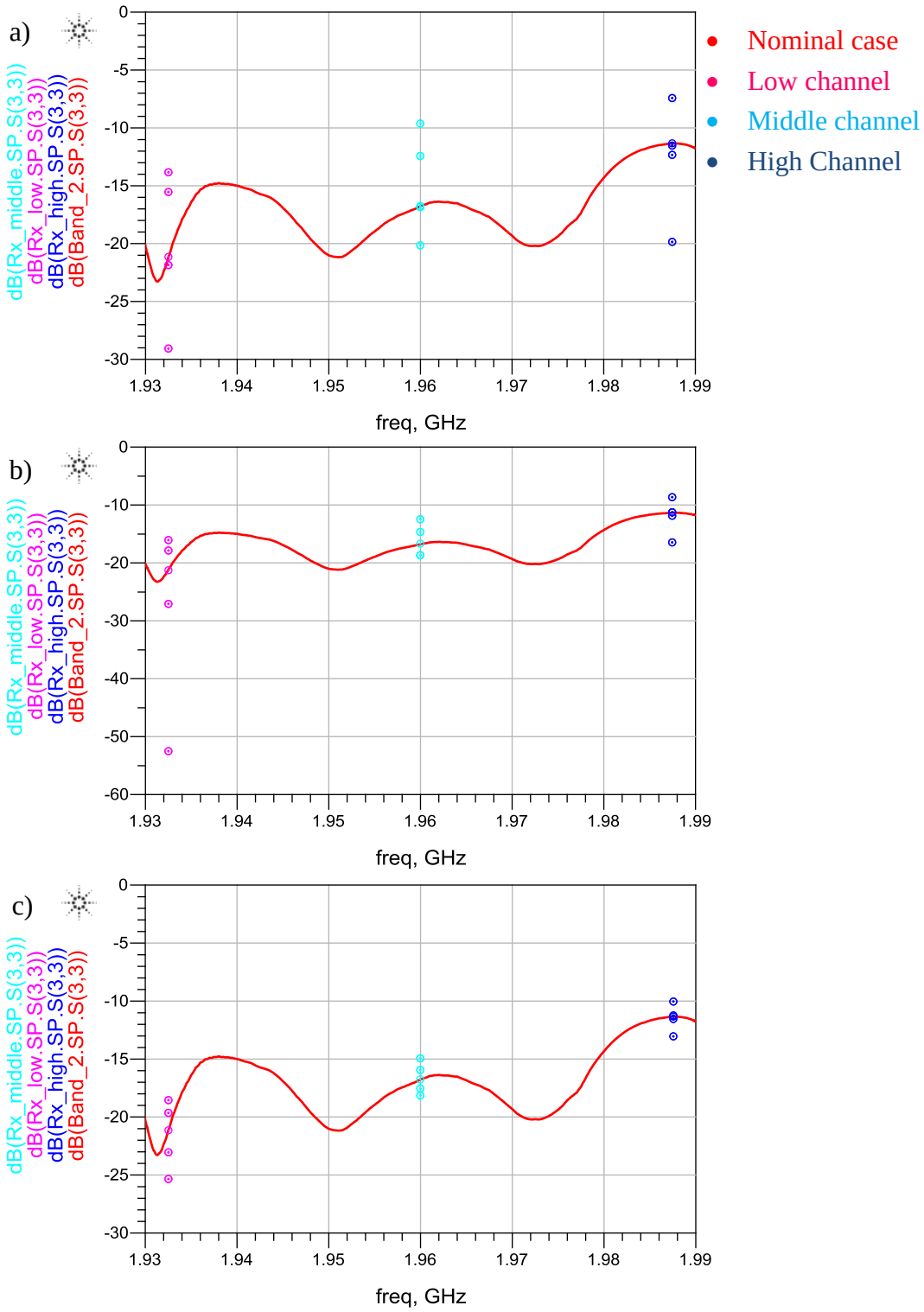

Figure 14. *Receiver return loss for LTE band 2 with a) ± 50 %, b) ± 25 %, and c) ± 10 % variation in transmission line lengths.*

It is noted that with ± 25 % limits, the variation at lower channel frequency is more than with ± 50 % limits. On other channels variation is decreasing from ± 50 % to ± 10 %.

Different variations from nominal results are gathered in Table 6. -Δ shows the maximum variation to negative direction, and +Δ shows the maximum variation to positive direction. If there is – sign, it shows that there is no variance to that direction.

Table 6. *Receiver return loss maximum variations in each limit case for LTE band 2.*

		± 50 %		**± 25 %**		**± 10 %**	
	Nominal (dB)	-Δ (dB)	+Δ (dB)	-Δ (dB)	+Δ (dB)	-Δ (dB)	+Δ (dB)
Low Channel	-21.176	8.006	7.336	31.528	5.150	4.143	2.627
Middle Channel	-16.745	3.406	6.752	1.915	4.199	1.452	1.763
High Channel	-11.347	8.474	3.798	5.093	2.714	1.703	1.312

Analysis showed that transmission line A has the greatest impact to variation on low and middle channel frequencies with all limit cases. On high channel transmission line B causes the most variation. Transmission line C has no effect to receiver return loss.

5.4 Uplink insertion loss

Next the uplink insertion loss, the attenuation from transmitter port to antenna port, is studied. Figure 15 illustrates the studied signal route on a block diagram.

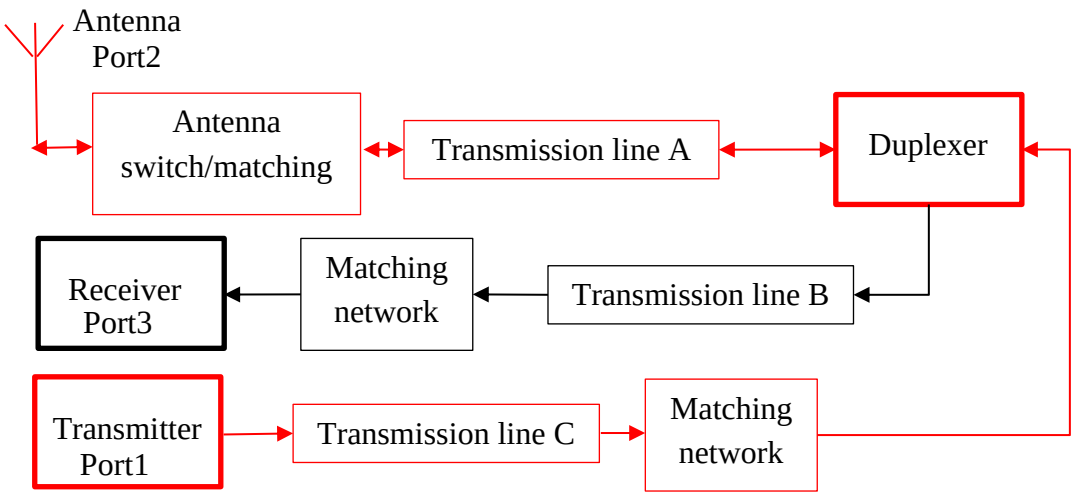

Figure 15. *Uplink insertion loss is measured as attenuation between ports 1 and 2.*

Figure 16 shows the variation in different limit cases.

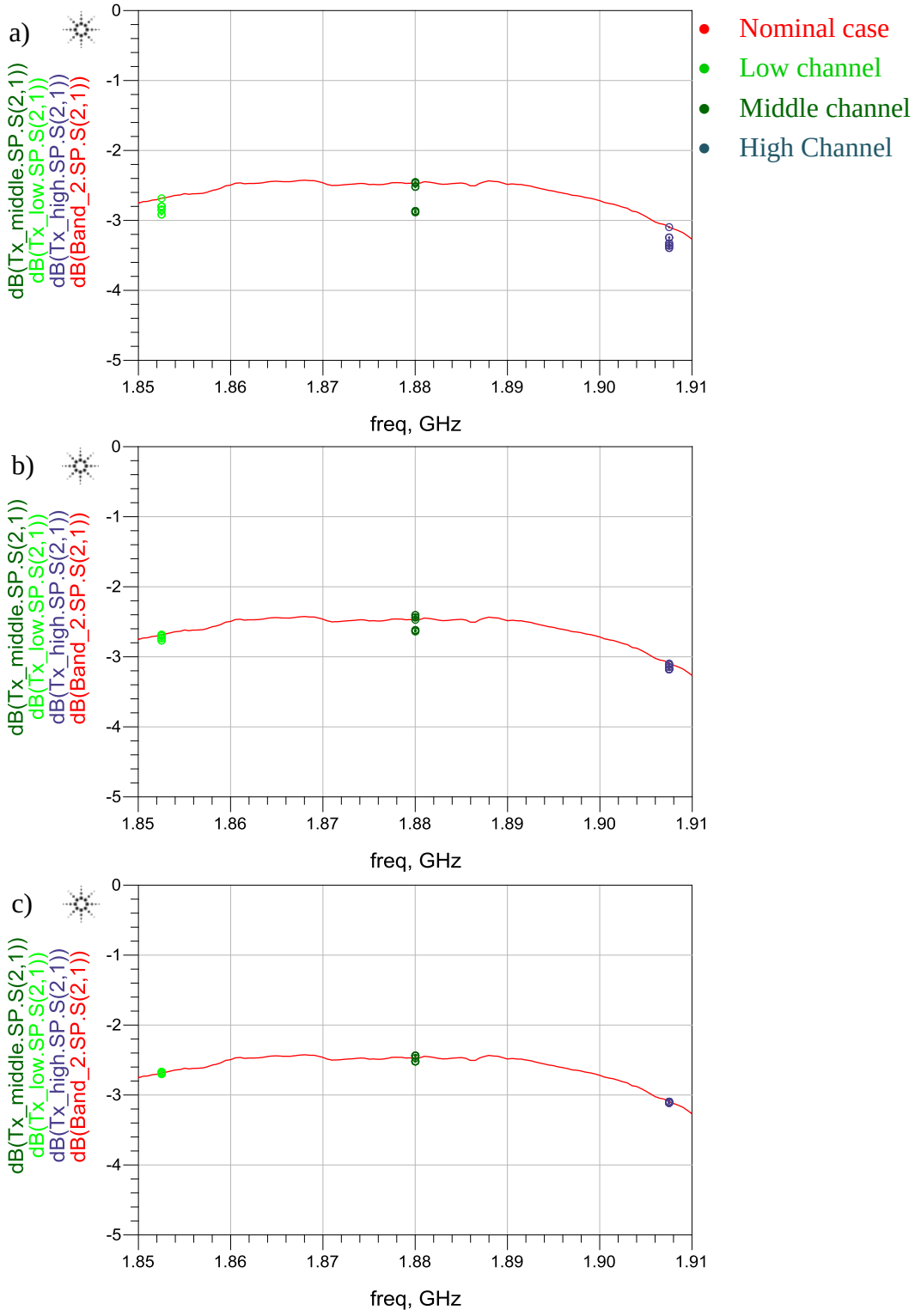

Figure 16. *Uplink insertion loss for LTE band 2 with a) ± 50 %, b) ± 25 %, and c) ± 10 % transmission line length variation.*

It is seen that variation decreases, and with ± 10 % limits there is only very minor variation from nominal results. Different variations from nominal results are gathered in Ta-

ble 7. -Δ shows the maximum variation to the negative direction, and +Δ shows the maximum variation in positive direction. If there is – sign, it shows that there is no variance to that direction.

Table 7. *LTE band 2 uplink insertion loss variations with each limit case.*

		± 50 %		**± 25 %**		**± 10 %**	
	Nominal (dB)	-Δ (dB)	+Δ (dB)	-Δ (dB)	+Δ (dB)	-Δ (dB)	+Δ (dB)
Low Channel	-2.682	0.238	-	0.079	-	0.021	0.006
Middle Channel	-2.468	0.421	-	0.161	0.057	0.052	0.036
High Channel	-3.093	0.307	-	0.089	-	0.020	0.002

Simulation revealed that transmission line A is the dominant transmission line on all studied frequencies. In addition it was noted that transmission line B has no effect.

5.5 Downlink insertion loss

Final output response studied with the LTE band 2 is downlink insertion loss, or the attenuation from antenna port to receiver port. Figure 17 illustrates the simulated S_{32} route on a block diagram.

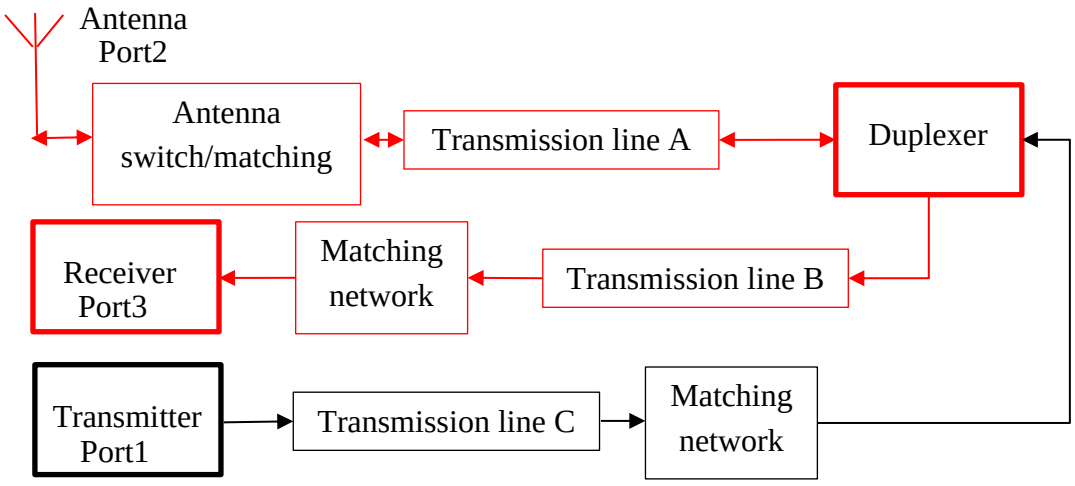

Figure 17. *Downlink insertion loss is measured as attenuation between ports 2 and 3.*

Figure 18 shows the variation in the downlink insertion loss with different limit cases.

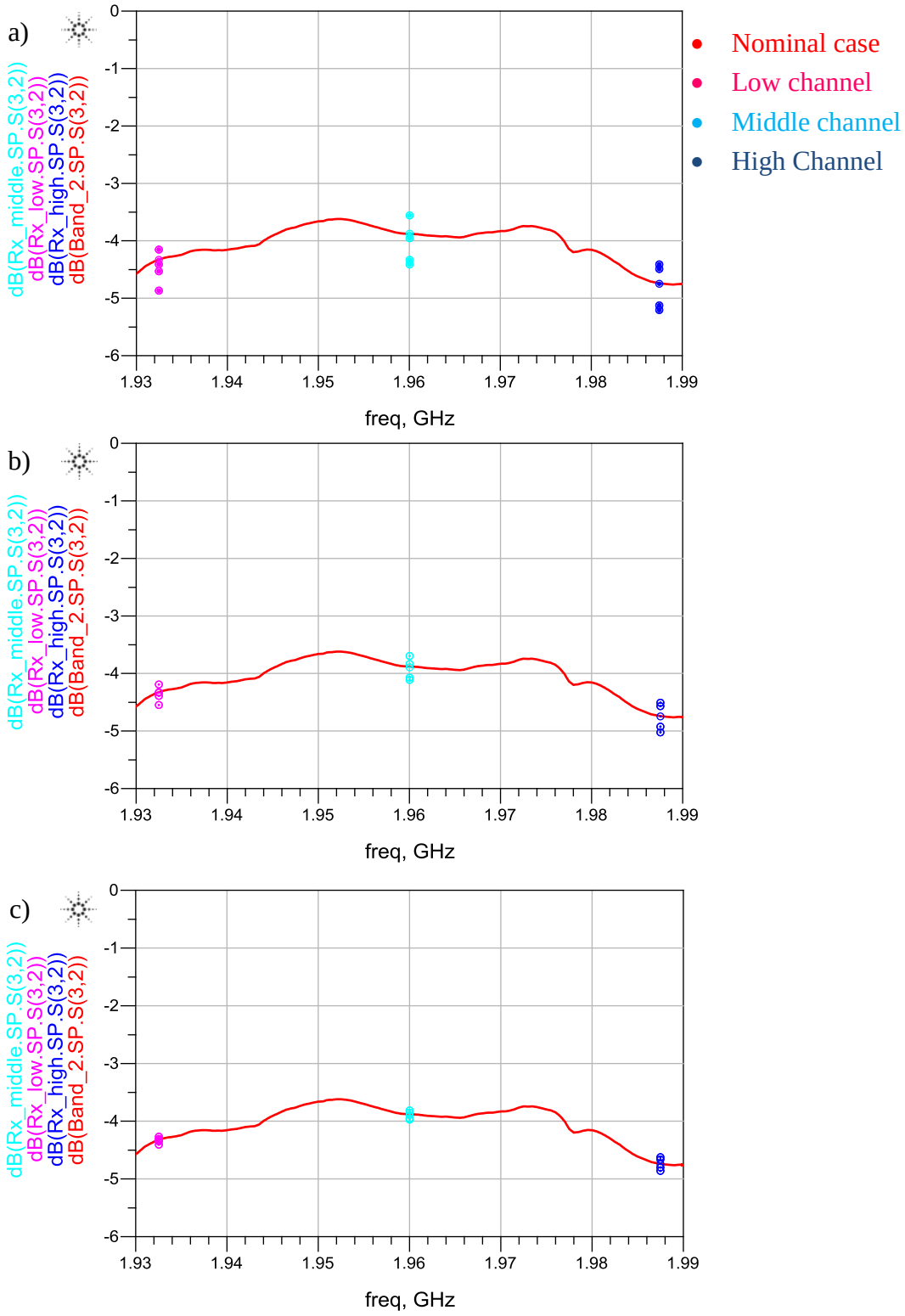

Figure 18. *LTE band 2 downlink insertion loss with a) ± 50 %, b) ± 25 %, and c) ± 10 % variation in transmission line lengths.*

Variation in insertion loss decreases from ± 50 % limit case to ± 10 % limit case. Different variations from nominal results are gathered in Table 8. -Δ shows the maximum variation to the negative direction, and +Δ shows the maximum variation to positive direction. If there is – sign, it shows that there is no variation to that direction.

Table 8. *Downlink insertion loss with different limits for LTE band 2.*

		± 50 %		**± 25 %**		**± 10 %**	
	Nominal (dB)	-Δ (dB)	+Δ (dB)	-Δ (dB)	+Δ (dB)	-Δ (dB)	+Δ (dB)
Low Channel	-4.325	0.547	0.194	0.227	0.126	0.078	0.062
Middle Channel	-3.885	0.477	0.319	0.233	0.182	0.086	0.078
High Channel	-4.740	0.390	0.335	0.290	0.235	0.121	0.112

Transmission line B has the greatest impact to variation on low channel frequencies. On middle and high channel the transmission line A is the dominating one. In addition, it is detected that transmission line C has no impact to downlink insertion loss variation.

5.6 Band 2 discussion

A common matter with all studied results and limit is that only up to five dots are visible at each frequency point. However, there are total of nine dots at each frequency point. One of the dots is on the red line and also represents the nominal situation. Excluding the nominal dot, each other points have duplicate entry. The reason for this is that transmission line B has no effect on studied uplink frequency outputs. Respectively, transmission line C has no effect on studied downlink frequency outputs. This happens due to the isolation the duplexer provides to separate the uplink and downlink frequency routes.

Transmitter return losses were presented in Table 4. Generally, point of interests here are the +Δ readings, as the matching goes poorer to that direction. It can be noted that variations are quite high throughout the different limits. However, that is to be expected as nominal results indicates that only a small amount of power is reflecting back to input. ± 10 % limits could be determined to be enough, as return loss is safely below -15 dB and relatively close to nominal results.

Antenna return losses were presented in Table 5. At uplink frequencies, it could be determined that ± 25 % limits are accurate enough on the same basis as in the uplink return loss case, though the difference to -15dB limit is not as big. At downlink frequencies, it might be necessary to have even more tighter limit. As the nominal value approaches -10 dB and above variation from nominal value becomes more important. Therefore, none of the limits could be used at downlink frequencies for antenna return loss.

Receiver return losses were gathered in Table 6. In this case, a ± 10 % limit could be implemented to stay below -10 dB return loss. On low and middle channels broader limit could also be allowed but the strictest limit must be chosen.

Different insertion loss cases were gathered in Table 7 at uplink route, and in Table 8 for downlink route. At uplink route ± 25 % limit could be chosen as the variation is very small. Same ± 25 % limit could also be chosen for the downlink route.

The limiting output for studied downlink frequencies is the antenna return loss, where none of the studied limits is sufficient. Simulation data suggests that transmission line A has the most contribution to variation. Therefore, it might be necessary to implement extra simulations to find out if ± 10 % limit could be used with transmission line B while tighter limits are applied to transmission line A.

Studied uplink frequency outputs have no limiting factor, and the smallest studied limit, ± 10 %, could be applied to transmission line C. As mentioned above, transmission line A might require tighter limit to remain the variation small enough on downlink route.

6. 700-MHZ BAND 12 DOE ANALYSIS

Transmission lines for band 12 are chosen as depicted in Figure 8. Transmission line lengths for band 12 with different limits are gathered in Table 9.

Table 9. *Transmission line lengths with each studied limit case for LTE-FDD band 12.*

Transmission line	Nominal (mm)	+50% (mm)	-50% (mm)	+25 % (mm)	-25% (mm)	+10% (mm)	-10% (mm)
ANT (A)	1.228	1.842	0.614	1.535	0.921	1.351	1.105
RX (B)	19.130	28.695	9.565	23.913	14.348	21.043	17.217
TX (C)	0.563	0.845	0.282	0.704	0.423	0.619	0.507

It can be noted that transmission lines A and C are both a lot shorter than transmission line B. The nominal case will also be simulated, as was the case with band 2, so the variation in each different limit case can be compared to it.

6.1 Transmitter return loss

Next the return loss of the transmitter is studied for band 12. The reference impedance is the ACLR optimum impedance point. Only uplink frequencies are studied in this case. Figure 19 shows the simulated port in the front end block diagram.

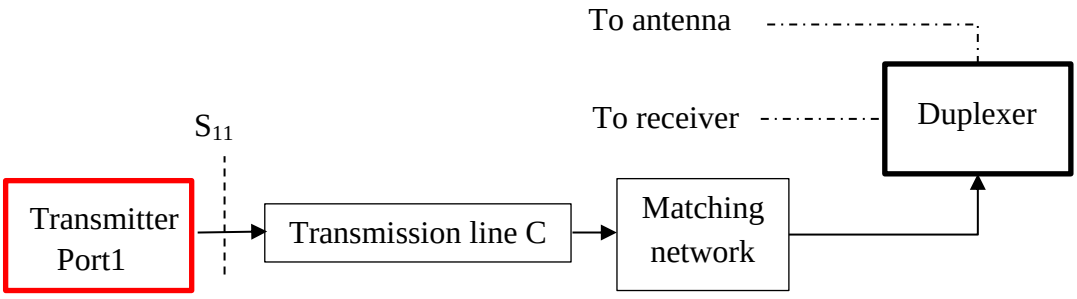

Figure 19. *Transmitter return loss is measured from port 1.*

Figure 20 shows the variation on studied frequency points when the length of transmission line is varied with different limits.

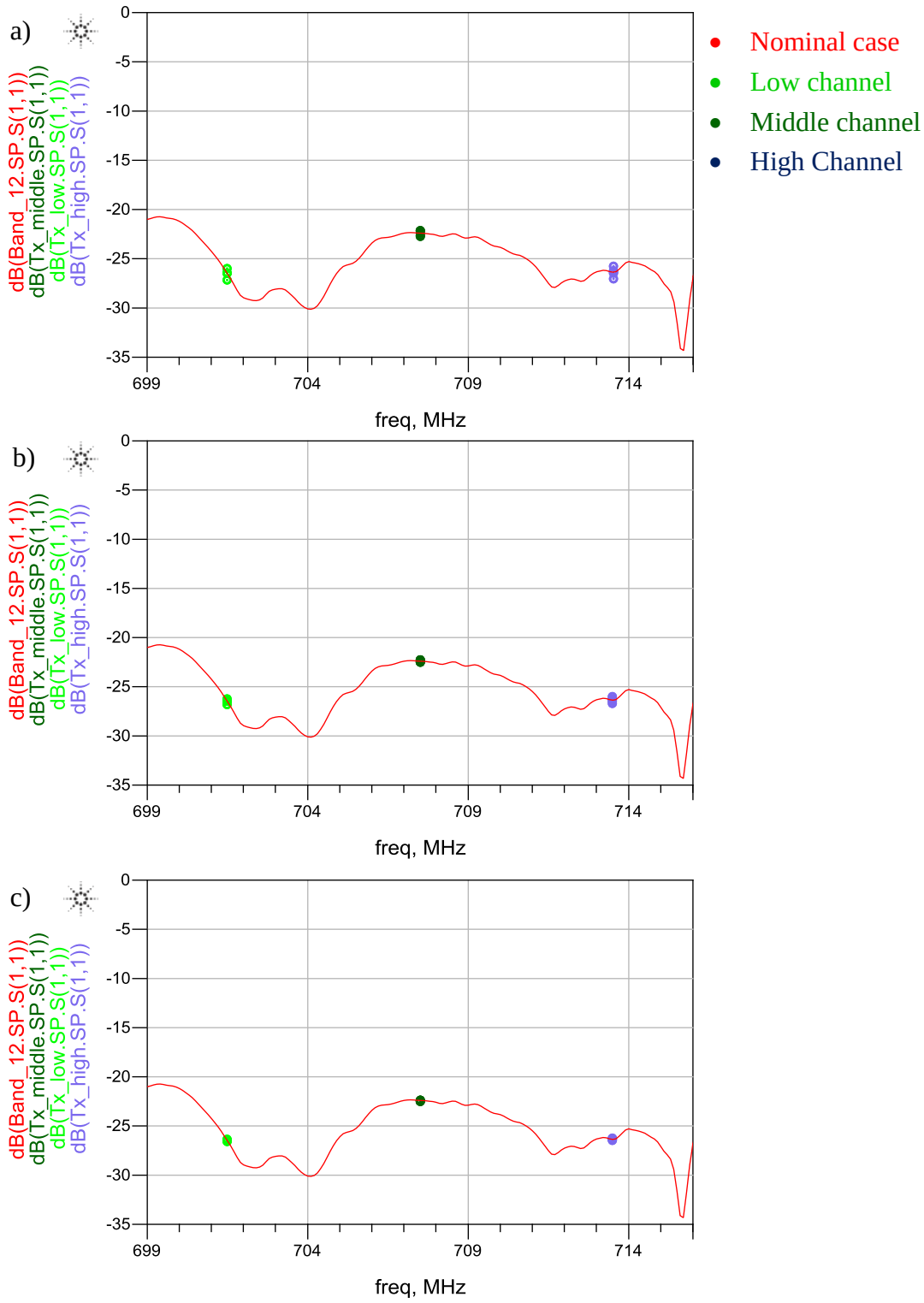

Figure 20. *LTE band 12 transmitter return loss variation with a) ± 50 %, b) ± 25 %, and c) ± 10 % variation in transmission line lengths.*

It is seen that only very minor variations are present with each limits. Negative and positive maximum variations are gathered in Table 10. -Δ shows the maximum variation to the negative direction, and +Δ shows the maximum variation to positive direction.

Table 10. *LTE band 12 transmitter return loss variations with different limits.*

		± 50 %		**± 25 %**		**± 10 %**	
	Nominal (dB)	-Δ (dB)	+Δ (dB)	-Δ (dB)	+Δ (dB)	-Δ (dB)	+Δ (dB)
Low Channel	-26.509	0.599	0.564	0.295	0.286	0.116	0.116
Middle Channel	-22.400	0.288	0.294	0.145	0.146	0.059	0.058
High Channel	-26.369	0.698	0.654	0.343	0.333	0.136	0.134

Transmitter return loss study revealed that transmission line A and C have nearly identical contribution to variation at low channel. At middle and high channel frequencies, and with all limit cases, transmission line A introduces the most variation.

6.2 Antenna return loss

Antenna return loss is studied with band 12 both uplink and downlink frequencies are studied. Figure 21 illustrates the port under study in a block diagram.

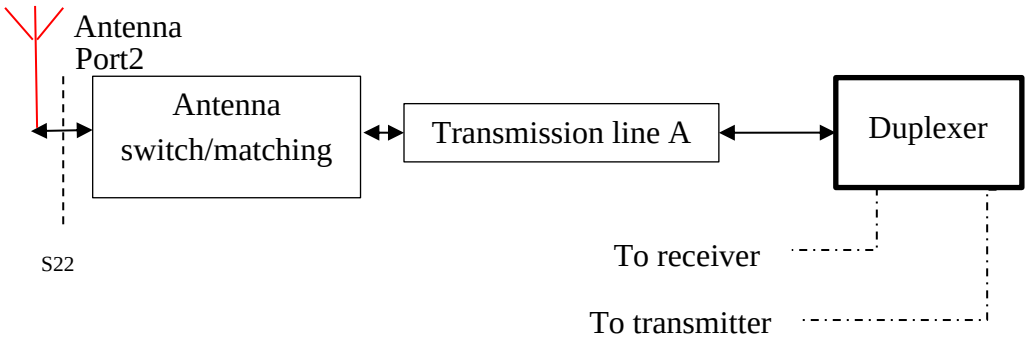

Figure 21. *Antenna return loss is measured from port 2.*

Figure 22 shows the variation in antenna return loss with different DOE limits.

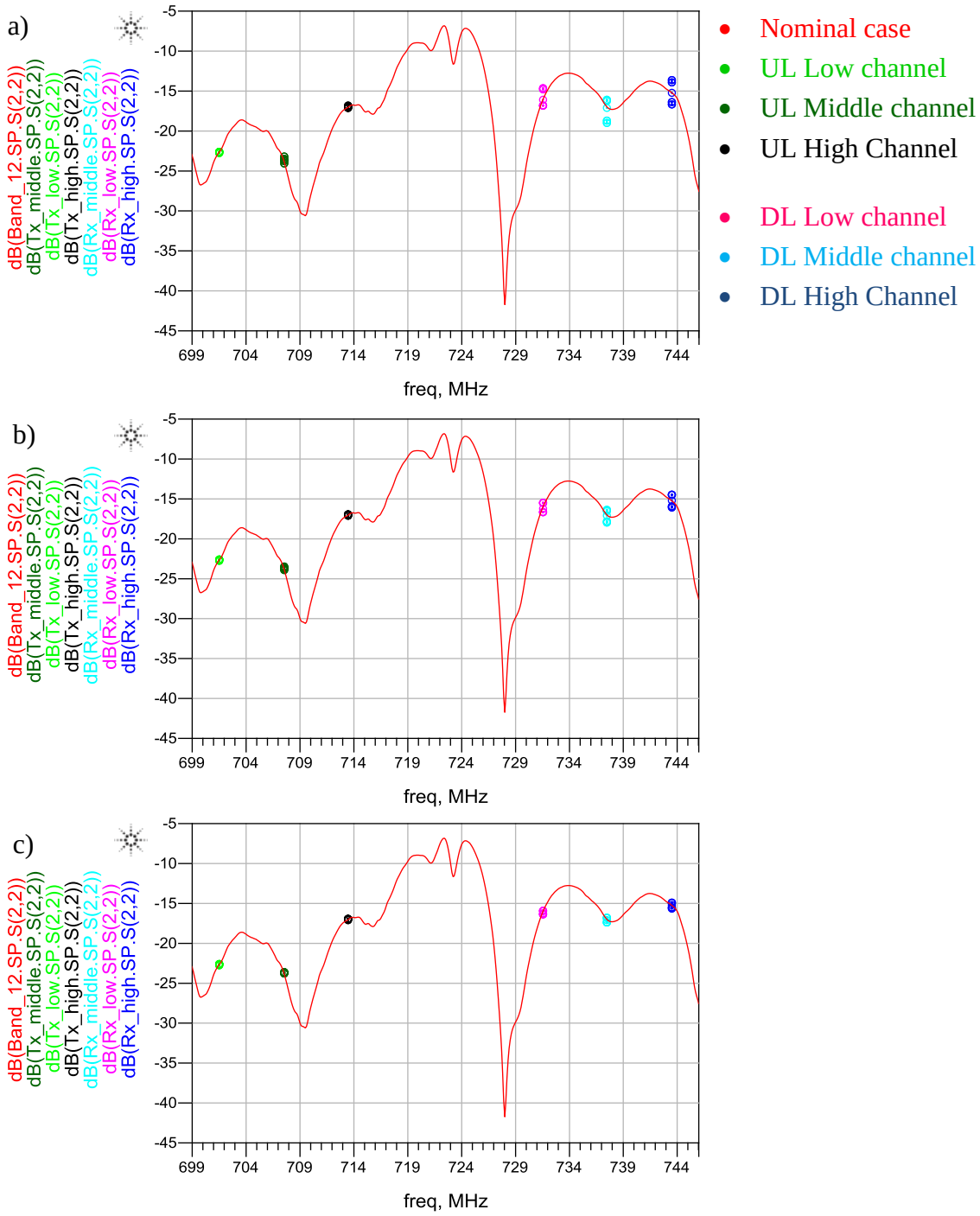

Figure 22. *LTE band 12 antenna return loss variations with a) 50 %, b) ± 25 %, and c) ± 10 % transmission line limits.*

Variation is greater in downlink frequencies, while in uplink frequencies there is only minor variation with each limit. Variations with each limit are gathered in Table 11.

Table 11. *Band 12 antenna return loss variation with different limits.*

			± 50 %		**± 25 %**		**± 10 %**	
		Nominal (dB)	-Δ (dB)	+Δ (dB)	-Δ (dB)	+Δ (dB)	-Δ (dB)	+Δ (dB)
Uplink	Low Channel	-22.66	0.087	0.091	0.044	0.045	0.018	0.018
	Middle Channel	-23.667	0.431	0.413	0.213	0.209	0.084	0.084
	High Channel	-16.994	0.130	0.127	0.065	0.064	0.026	0.026
Downlink	Low Channel	-16.153	0.618	1.492	0.504	0.722	0.238	0.274
	Middle Channel	-17.049	1.989	0.983	0.854	0.606	0.310	0.271
	High Channel	-15.262	1.413	1.605	0.807	0.839	0.335	0.339

Transmission line A contributes most to variation on uplink channel frequencies. At all downlink channel frequencies transmission line C introduces the most variation.

6.3 Receiver return loss

Receiver return loss for band 12 is studied with downlink frequencies. The reference impedance is the noise optimum impedance, similar to band 2 simulations. Figure 23 highlights the simulated port in a block diagram.

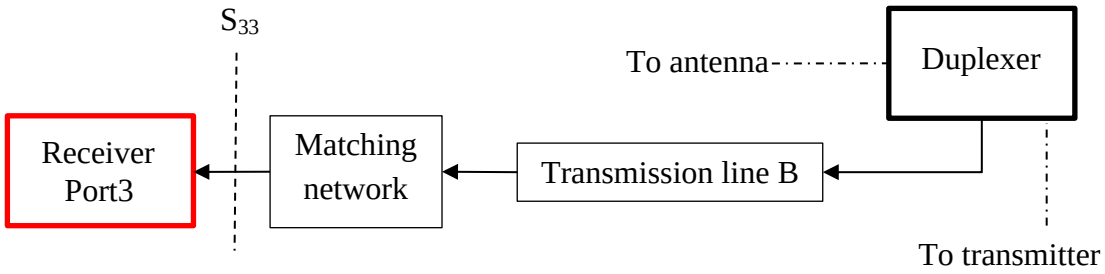

Figure 23. *Receiver return loss is measured from port 3.*

Figure 24 shows the variation in downlink low, middle, and high channels.

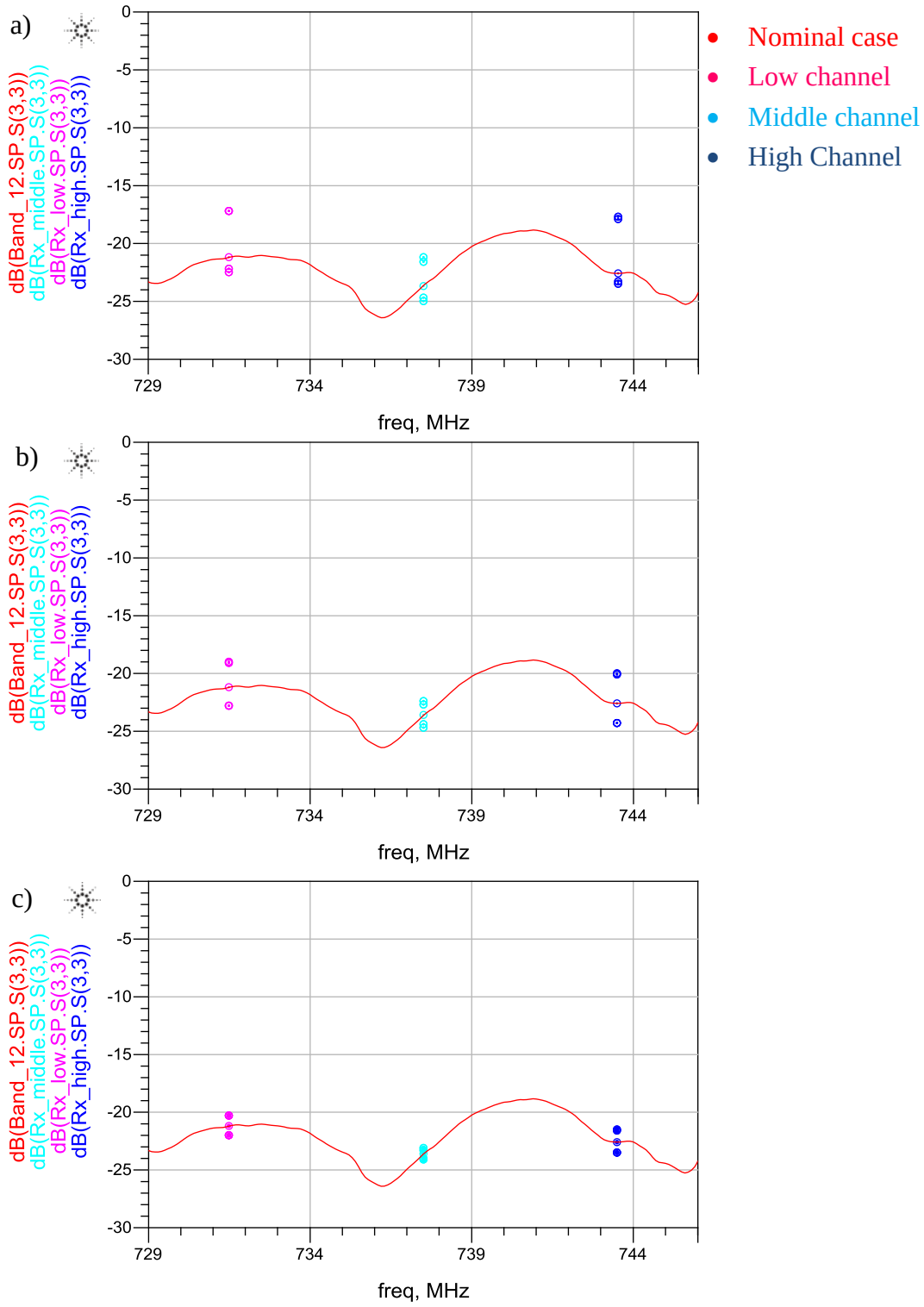

Figure 24. *Receiver return loss variation for LTE band 12 with a) ± 50 %, b) ± 25 %, and c) ± 10 % limit.*

It is seen that variation decreases with studied frequency points when the limits go from ± 50 % to ± 10 %. Band 12 receiver return loss variations from nominal results are gathered in Table 12.

Table 12. *Negative and positive maximum variations for band 12 receiver return loss.*

		± 50 %		**± 25 %**		**± 10 %**	
	Nominal (dB)	-Δ (dB)	+Δ (dB)	-Δ (dB)	+Δ (dB)	-Δ (dB)	+Δ (dB)
Low Channel	-21.197	1.283	4.045	1.626	2.166	0.797	0.873
Middle Channel	-23.639	1.317	2.446	1.010	1.255	0.459	0.495
High Channel	-22.579	0.983	4.845	1.716	2.592	0.922	1.039

Transmission line B contributes the most to the variation from nominal results. This is the case with low, middle, and high channel frequencies on each limit case.

6.4 Uplink insertion loss

Next, the insertion loss from transmitter to antenna is studied. The simulated signal route is illustrated in Figure 25.

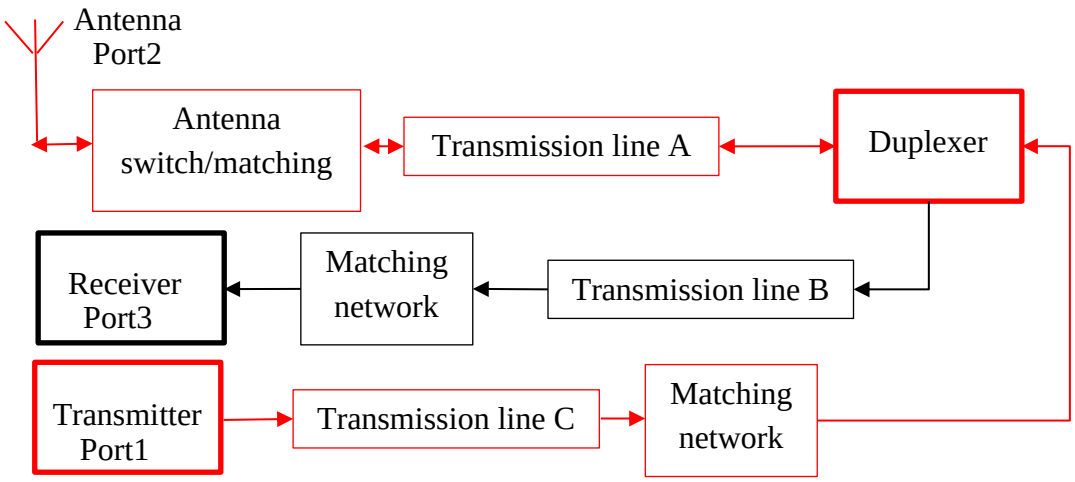

Figure 25. *Uplink insertion loss is measured as attenuation between ports 1 and 2.*

Figure 26 shows the uplink insertion loss with the three limits used.

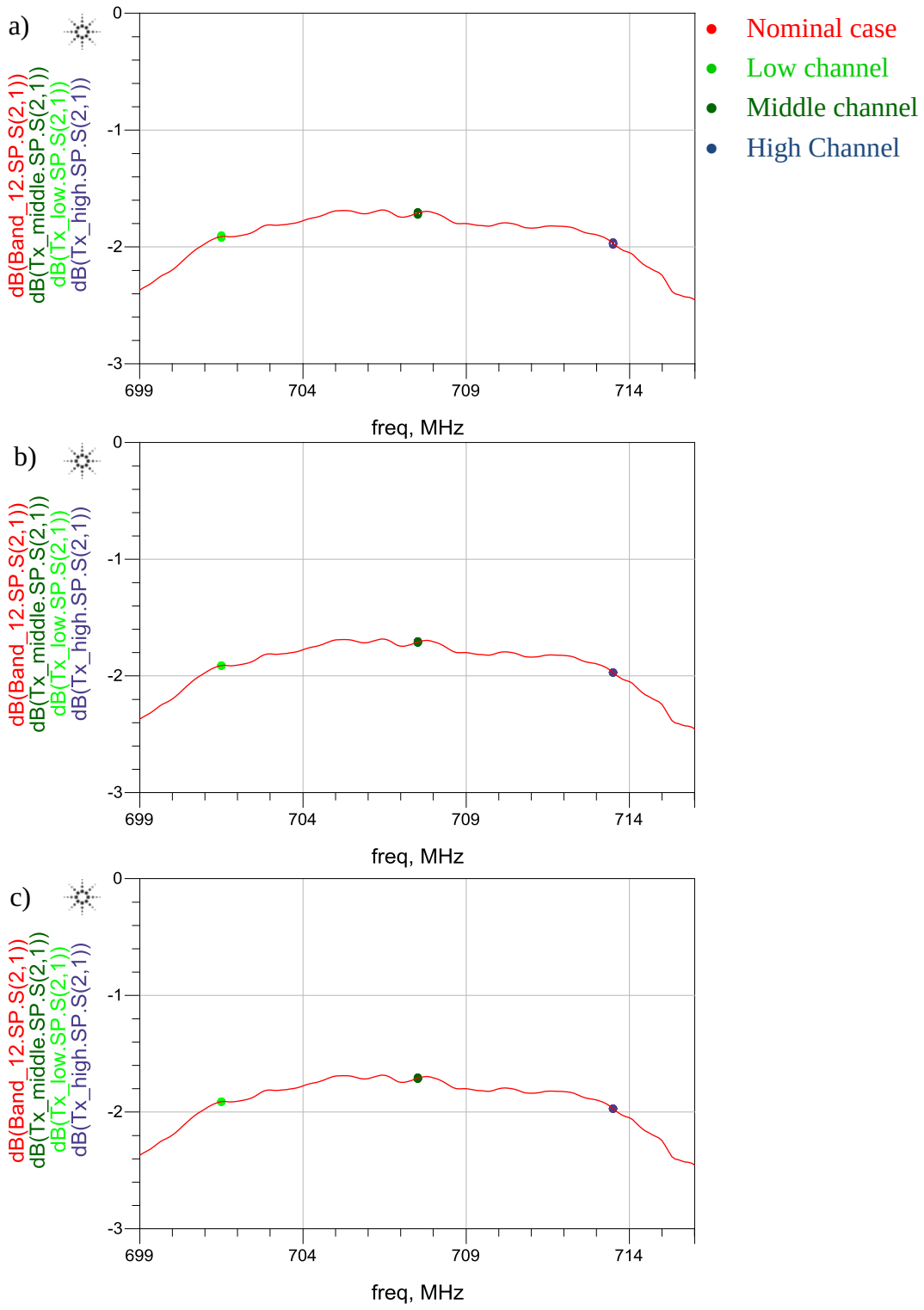

Figure 26. *LTE band 12 uplink insertion loss variations with a) 50 %, b) ± 25 %, and c) ± 10 % limit case.*

It is seen that only very minor variation from nominal results are received with each limit. Different variations from nominal results in the uplink insertion loss are gathered in Table 13.

Table 13. *Uplink insertion loss variations from nominal results with LTE band 12.*

		± 50 %		**± 25 %**		**± 10 %**	
	Nominal (dB)	-Δ (dB)	+Δ (dB)	-Δ (dB)	+Δ (dB)	-Δ (dB)	+Δ (dB)
Low Channel	-1.911	0.008	0.008	0.004	0.004	0.001	0.002
Middle Channel	-1.711	0.010	0.010	0.005	0.005	0.002	0.002
High Channel	-1.970	0.007	0.006	0.004	0.003	0.002	0.001

Transmission line A introduces the most variation at low and middle channel frequencies. At high channel frequencies, transmission lines A and C are the main cause of variation.

6.5 Downlink insertion loss

Last output studied for LTE band 12 is the insertion loss from antenna to receiver. Figure 27 shows the simulated path.

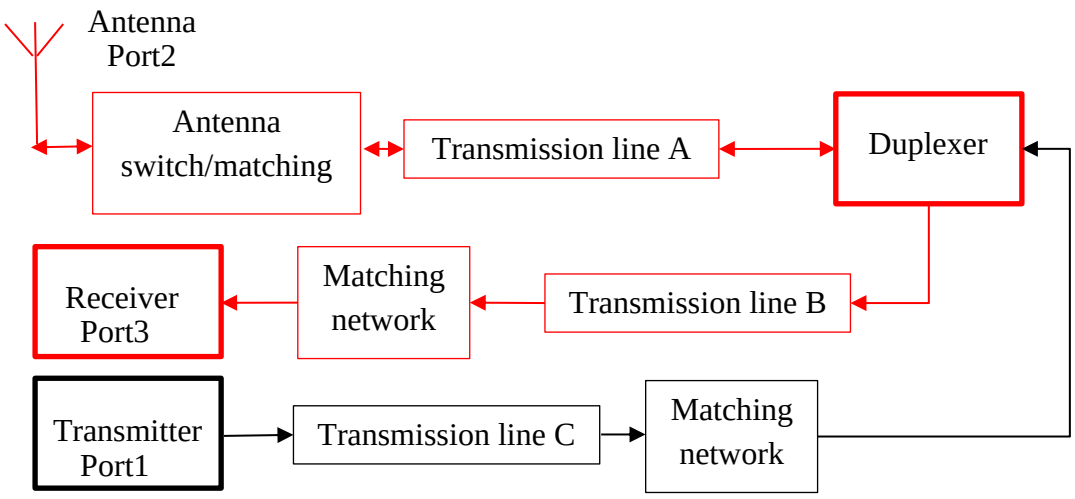

Figure 27. *Downlink insertion loss is measured as attenuation between ports 2 and 3.*

Figure 28 illustrates the downlink insertion loss.

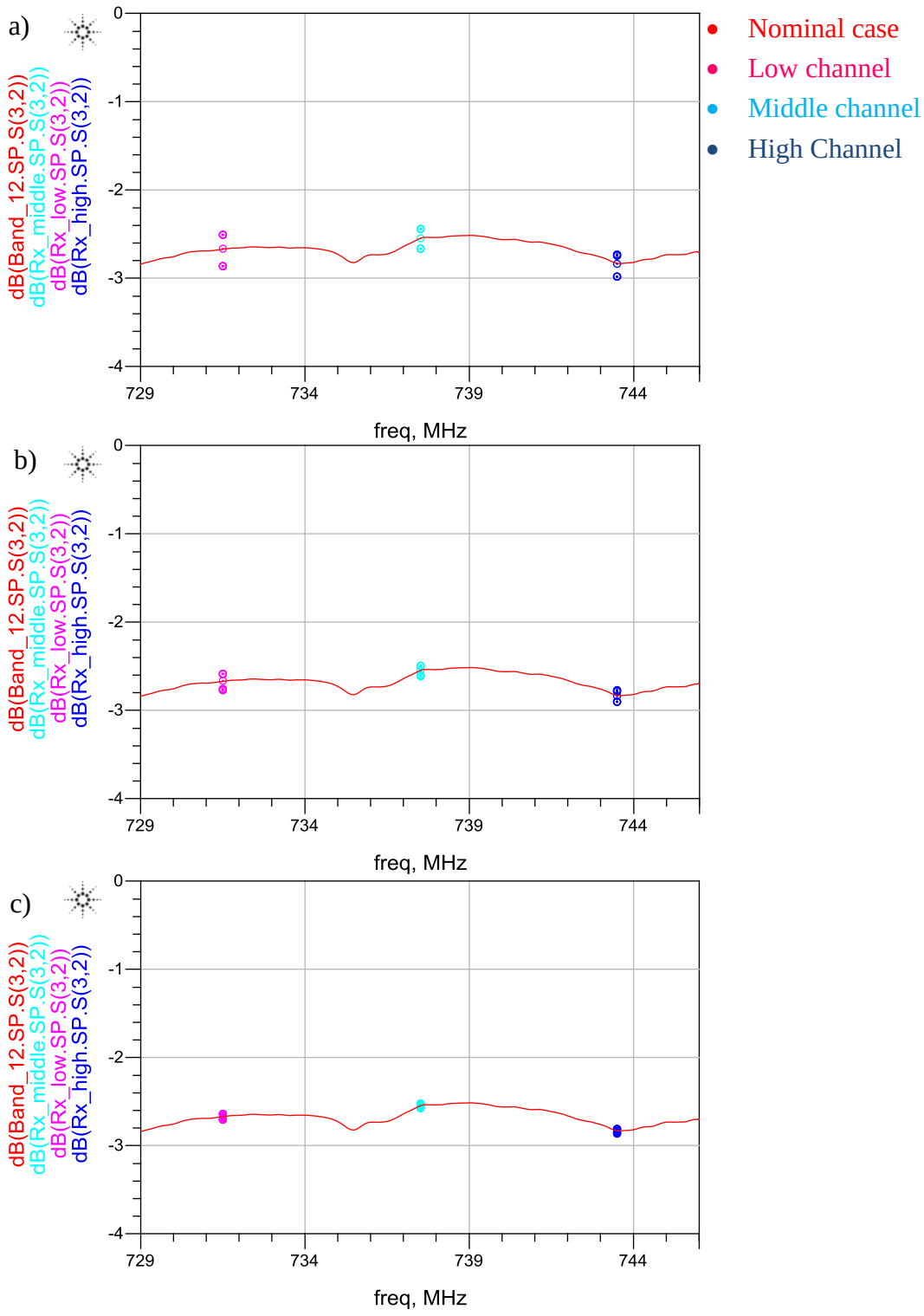

Figure 28. *Downlink insertion loss variations for LTE band 12 with a) ± 50 %, b) ± 25 %, and c) ± 10 % limit case.*

It is seen that variation decreases as limits are gradually changed from ± 50 % to ± 10 %. Negative and positive maximum variations are stored in Table 14.

Table 14. *LTE band 12 downlink insertion loss variations with different limits.*

		± 50 %		**± 25 %**		**± 10 %**	
	Nominal (dB)	-Δ (dB)	+Δ (dB)	-Δ (dB)	+Δ (dB)	-Δ (dB)	+Δ (dB)
Low Channel	-2.673	0.196	0.168	0.097	0.089	0.038	0.037
Middle Channel	-2.551	0.119	0.107	0.058	0.055	0.023	0.023
High Channel	-2.833	0.151	0.101	0.070	0.057	0.027	0.024

Simulations revealed that transmission line B introduces the most variation from nominal results. However, it should be noted that variation remains relatively small through all channel frequencies and limit cases.

6.6 Band 12 discussion

All studied uplink frequency outputs (presented in Table 10, Table 11, and Table 13) show hardly any variation with the different limits. Reasons for this are the relatively short transmission line lengths that are in the uplink route. Therefore, ± 50 % or even wider limits could be applied to the studied uplink frequency outputs. However, transmission line A is used in both uplink and downlink routes.

Antenna return losses were presented in Table 11. For uplink it is already mentioned that ± 50 % limits could be applied. For downlink it seems that more suitable would be to apply ± 25 % limit, where the variation remains small enough.

Downlink return losses were presented in Table 12. It is seen that variation is yet quite large on ± 50 % limits. However, the matching still remains under the -15 dB. Therefore, the ± 50 % limits could be used for downlink return loss.

Downlink insertion losses were presented in Table 14. Maximum variation is 0.2 dB from nominal result with ± 50 % limit. In this case it can be determined to be enough.

Now, the limiting output is antenna return loss at downlink frequencies. Therefore, ± 25 % would have to be chosen based on these results for transmission line A and B, and ± 50 % could be applied to transmission line C. However, as simulation data suggests that

transmission line B contributes the most, ± 50 % limit could be considered for transmission line A.

7. CONCLUSION

The purpose of this thesis was to study if DOE can be applied to RF design process. DOE was applied to study the effects of transmission line lengths. Existing simulation models were used to perform the study. Different limits where tested to research the effects of transmission line lengths to find out what limits would have been adequate in each case.

DOE was conducted on two different LTE-FDD front ends, band 2 and band 12. Three different limits were applied to transmission line lengths (input factors). Transmission lines were positioned as depicted in Figure 8 for both studied front ends. Impacts of the length of the transmission lines to different outputs were examined. The outputs were defined as transmitter return loss, antenna return loss, receiver return loss, uplink insertion loss, and downlink insertion loss. Uplink and downlink frequencies were investigated on their respective outputs, and three points of interest were chosen for both uplink and downlink frequencies. Points of interest were decided to be low, middle, and high channel frequencies in both uplink and downlink frequencies.

After the DOE analysis for both bands it can be concluded that DOE could be applied to search for adequate limits for the transmission line lengths. However, in some cases not all the studied limits were accurate enough. This would mean that stricter limits might be required in certain cases. Another issue to consider is that if too strict limits are required the limits may not be feasible in a real life situation. For example, if 20 mm (assuming it would be close to nominal length) transmission line has to be defined with ± 5% limits (± 1 mm), it may prove very difficult to apply that length in layout depending on the complexity of the signal route. On the other hand, if wide limits can be applied to short transmission line lengths applicability to layout should be easy enough. For instance, if a 0.5 mm transmission line can be defined with ± 50 % (± 0.25 mm) limits, it should be trivial to apply as no complex signal routes are to be expected.

It was not possible to determine same percentual limits to all transmission line lengths so that variation would remain small. This may increase the challenge in defining initial limits and their usability to simulations. In addition, different front end signal routes use their unique key component and matching solutions. Therefore, each front end signal route may need their own distinctive limits.

In practice, upper and lower limits can be received from the draft layout. DOE can then be applied to verify whether the variation in performance parameters is acceptable. If variation is small enough, further simulations could be performed. In the case that varia-

tion is too large two options are possible: wait until more accurate limits are possible, or wait that layout is completed on that part and real value of transmission line length is used. DOE applicability may be limited by the upper and lower limits in use.

In similar manner, the DOE could also be applied to other technologies, such as GSM or WCDMA front end transmission lines. DOE is not limited only to RF front ends. It might also be appropriate tool to analyze transmission lines in other areas in mobile design, for instance transmission lines between different ICs.

Further DOE analysis could also be performed to widths of the transmission line. Using same method the effects of the transmission line widths could be studied. It might also be possible to find out the optimal width for each transmission line.

REFERENCES

[1] "3GPP Specifications," 3GPP, A Global Initiative, 27 March 2014. [Online]. Available: http://www.3gpp.org/specifications/specifications. [Accessed 26 March 2015].

[2] D. M. Pozar, Microwave Engineering 3rd edition, John Wiley & Sons, Inc., 2005, 700 p.

[3] R. Behzad, RF Microelectronics, Prentice-Hall, Inc., 1998, 335 p.

[4] B. Razavi, Design of Analog CMOS Integrated Circuits, International Edition, McGraw-Hill Companies, 2001, 648 p.

[5] ETSI, "ETSI TS 136 104 V10.2.0 (2011-05) - Technical specification," [Online]. Available: http://www.etsi.org/deliver/etsi_TS/136100_136199/136104/10.02.00_60/ts_136104v100200p.pdf. [Accessed 18 May 2015].

[6] S. C. Cripps, RF Power Amplifiers for Wireless Communications, Archtech House, Inc., 1999, 337 p.

[7] M. Lapinoja and T. Rahkonen, "An active tuning and impedance matching element," *Circuits and Systems, 1998. ISCAS '98. Proceedings of the 1998 IEEE International Symposium on,* vol. 1, pp. 559-562, 1998.

[8] 3GPP, "LTE," [Online]. Available: http://www.3gpp.org/technologies/keywords-acronyms/98-lte. [Accessed 20 May 2015].

[9] D. Trends, "What's the difference between 4G and LTE?," [Online]. Available: http://www.digitaltrends.com/mobile/4g-vs-lte/. [Accessed 18 May 2015].

[10] "ETSI TR 125 913 V7.3.0," 3GPP, 2013.

[11] I. Poole, "OFDM Orthogonal Frequency Dicision Multiplexing Tutorial," [Online]. Available: http://www.radio-electronics.com/info/rf-technology-design/ofdm/ofdm-basics-tutorial.php. [Accessed 12 May 2015].

[12] I. Poole, "3G LTE Long Term Evolution Tutorial & Basics," Radio-Electronics.com, [Online]. Available: http://www.radio-electronics.com/info/cellulartelecomms/lte-long-term-evolution/3g-lte-basics.php.

[Accessed 26 March 2015].

[13] I. Poole, "LTE OFDM, OFDMA SC-FDMA & Modulation," [Online]. Available: http://www.radio-electronics.com/info/cellulartelecomms/lte-long-term-evolution/lte-ofdm-ofdma-scfdma.php. [Accessed 12 May 2015].

[14] I. Poole, "LTE FDD, TDD, TD-LTE Duplex Schemes," Radio-Electronics.com, [Online]. Available: http://www.radio-electronics.com/info/cellulartelecomms/lte-long-term-evolution/lte-fdd-tdd-duplex.php. [Accessed 26 March 2015].

[15] Keysight Technologies, "Using Design of Experiments (DOE)," [Online]. Available: http://edadocs.software.keysight.com/display/ads2009/Using+Design+of+Experiments+%28DOE%29. [Accessed 13 May 2015].

[16] NIST/SEMATECH, "5.1.1. What is experimental design?, Engineering Statistics Handbook," 30 October 2013. [Online]. Available: http://www.itl.nist.gov/div898/handbook/pri/section1/pri11.htm. [Accessed 8 May 2015].

[17] Keysight, "Design of Experiments (DOE) Tutorial," [Online]. Available: http://www.keysight.com/upload/cmc_upload/All/DesignOfExperimentsTutorial.pdf. [Accessed 12 May 2015].

[18] "Design of Experiments (DOE)," MoreSteam, [Online]. Available: https://www.moresteam.com/toolbox/design-of-experiments.cfm. [Accessed 8 May 2015].

[19] NIST/SEMATECH, "5.3.3.4.6 Screening designs, Engineering Statistics Handbook," 30 October 2013. [Online]. Available: http://www.itl.nist.gov/div898/handbook/pri/section3/pri3346.htm. [Accessed 8 May 2015].

[20] D. Kroese, T. Taimre and Z. Botev, Hand Book of Monte Carlo Methods, 1st Edition, John Wiley & Sons Inc., 2011, 772 p.

[21] Agilent, "Using Statistical Design," [Online]. Available: http://cp.literature.agilent.com/litweb/pdf/ads2008/optstat/ads2008/Using_Statistical_Design.html. [Accessed 12 May 2015].

[22] 3GPP, "ETSI TS 136 106, Technical Specification," [Online]. Available: http://www.etsi.org/deliver/etsi_ts/136100_136199/136106/10.00.00_60/ts_13610

6v100000p.pdf. [Accessed 8 May 2015].